Published for SISSA by Springer

Received: November 7, 2011
Accepted: January 15, 2012
Published: February 7, 2012

J/ψ and ψ(2S) production in pp collisions at $\sqrt{s} = 7$ TeV

The CMS collaboration

Abstract: A measurement of the J/ψ and ψ(2S) production cross sections in pp collisions at $\sqrt{s} = 7$ TeV with the CMS experiment at the LHC is presented. The data sample corresponds to an integrated luminosity of 37 pb^{-1}. Using a fit to the invariant mass and decay length distributions, production cross sections have been measured separately for prompt and non-prompt charmonium states, as a function of the meson transverse momentum in several rapidity ranges and integrated in the kinematical regions considered in this study. In addition, cross sections restricted to the acceptance of the CMS detector are given, which are not affected by the polarization of the charmonium states. The ratio of the differential production cross sections of the two states, where systematic uncertainties largely cancel, is also determined. The branching fraction of the inclusive $B \to \psi(2S)X$ decay is extracted from the ratio of the non-prompt cross sections to be:

$$\mathcal{B}(B \to \psi(2S)X) = (3.08 \pm 0.12\,(\text{stat.+syst.}) \pm 0.13\,(\text{theor.}) \pm 0.42\,(\mathcal{B}_{\text{PDG}})) \times 10^{-3}.$$

Keywords: Hadron-Hadron Scattering

doi:10.1007/JHEP02(2012)011

JHEP02(2012)011

Contents

JHEP02(2012)011

1 Introduction

Quarkonium production at hadron colliders provides important tests of calculations in the context of both perturbative and non-perturbative quantum chromodynamics (QCD), via measurements of production cross sections and polarizations.

The J/ψ and $\psi(2S)$ mesons can be produced in proton-proton (pp) collisions through two mechanisms: prompt mesons directly produced in the primary interaction and non-prompt mesons from the decay of directly produced b hadrons. In addition, J/ψ production can also occur via decays of heavier charmonium states, both S-wave (the $\psi(2S)$ itself) and P-wave (the three χ_c states). The determination of the latter contribution is challenging both theoretically and experimentally, because it requires detection of the low-energy

photons from χ_c decays. In nonrelativistic QCD (NRQCD) models [1, 2], by adding a contribution to prompt charmonium production through colour-octet states [3], a satisfactory description of prompt J/ψ and $\psi(2S)$ meson cross sections at the Tevatron [4] has been obtained. However, in these calculations the fraction of J/ψ originating from χ_c decays must be assumed from experimental measurements with large uncertainties, which makes the $\psi(2S)$ mesons cleaner probes of NRQCD predictions.

Non-prompt J/ψ and $\psi(2S)$ production can be directly related to b-hadron production, providing a measurement of the b-hadron cross section in pp collisions. Past discrepancies between the Tevatron results and the next-to-leading-order (NLO) QCD calculations have been resolved using the fixed-order next-to-leading-log (FONLL) approach and updated measurements of the $b \to J/\psi$ fragmentation and decay [5, 6].

Measurements of the prompt and non-prompt production cross sections of J/ψ mesons decaying to muon pairs was published using the first Compact Muon Solenoid (CMS) data [7], as well as data from other LHC experiments [8–10]. The present analysis extends the CMS result with a larger amount of statistically independent data and complements it by providing a measurement of the $\psi(2S)$ production cross section, as well as the ratio of the two cross sections. Higher trigger thresholds induced by the increased LHC luminosity do not allow the current measurement to reach charmonium transverse-momentum (p_T) values as low as in ref. [7], but the high-p_T reach is increased by the much larger amount of data. The advantage of measuring the $\psi(2S)$ to J/ψ cross section ratio lies in the cancellation of several experimental and theoretical uncertainties.

The polarizations of the J/ψ and $\psi(2S)$ states affect the muon momentum spectrum in the laboratory frame, thus influencing the charmonium acceptance and, as a consequence, the extracted cross sections. Therefore it was decided to present the results in two different ways. The first approach assumes unpolarized production for prompt J/ψ and $\psi(2S)$ whereas non-prompt mesons are assumed to have the polarization generated by the EvtGen Monte Carlo program [11], corrected to match the most recent measurements [12]. Typical changes of the measured cross sections resulting from using hypotheses of full longitudinal or full transverse polarizations are also given. The second approach provides results restricted to the phase-space region of the CMS muon detector acceptance, in order to avoid corrections which depend on the unknown polarizations of the two charmonium states.

The paper is structured as follows. In section 2 the analysis technique used to determine cross sections is briefly outlined. In section 3, a brief description of the CMS detector is provided. In section 4, the data and Monte Carlo samples are presented, and the event selection is described, while section 5 presents the method to extract the total J/ψ and $\psi(2S)$ yields. In section 6, corrections for acceptance and efficiency are explained, which are used to determine the inclusive cross sections, as discussed in section 7. Section 8 describes the method to extract the J/ψ and $\psi(2S)$ non-prompt fractions of the total yields. In section 9, the results of the differential cross sections, the non-prompt fractions, the cross section ratios, and the inclusive branching fraction $\mathcal{B}(B \to \psi(2S)X)$ from the ratio of the non-prompt cross sections are given.

JHEP02(2012)011

2 Cross section determination

Experimentally, the J/ψ double-differential cross section is given by:

$$\frac{\mathrm{d}^2\sigma}{\mathrm{d}p_\mathrm{T}\mathrm{d}y}(J/\psi)\cdot\mathcal{B}(J/\psi\to\mu^+\mu^-)=\frac{N^{\mathrm{corr}}_{J/\psi}(p_\mathrm{T},|y|)}{\int L\,\mathrm{d}t\cdot\Delta p_\mathrm{T}\cdot\Delta y}\quad , \tag{2.1}$$

where $\int L\,\mathrm{d}t$ is the integrated luminosity, Δp_T and Δy are the p_T and y bin widths, $\mathcal{B}(J/\psi\to\mu^+\mu^-)$ is the decay branching fraction of the J/ψ into two muons, and $N^{\mathrm{corr}}_{J/\psi}(p_\mathrm{T},|y|)$ is the corrected J/ψ yield in a given $(p_\mathrm{T},|y|)$ bin. The uncorrected signal yield $N_{J/\psi}$ is obtained through event selections and fits performed to invariant mass distributions. The corrected yield is obtained from $N_{J/\psi}$ via $N^{\mathrm{corr}}_{J/\psi}=N_{J/\psi}\cdot\langle\frac{1}{A\cdot\epsilon}\rangle_{\mathrm{bin}}$ in the case where the J/ψ yields are corrected for acceptance (A) and efficiency (ϵ), and $N^{\mathrm{corr}}_{J/\psi}=N_{J/\psi}\cdot\langle\frac{1}{\epsilon}\rangle_{\mathrm{bin}}$ in the case where the results are uncorrected for acceptance. The definition of acceptance and efficiency averages in p_T-$|y|$ bins is given in section 6. An analogous formula applies for the $\psi(2\mathrm{S})$ double-differential cross section.

Because of the large difference in the branching fractions to dimuons of the two states, the measured $\psi(2\mathrm{S})$ yield is much smaller than the J/ψ yield. For this reason, different binnings are used for the differential cross sections in p_T and $|y|$. The total p_T-$|y|$ range considered for the J/ψ cross sections is:

$$\begin{aligned}
&8.0<p_\mathrm{T}<70.0\ \mathrm{GeV}/c\ \ \text{for}\ \ |y|<0.9\\
&8.0<p_\mathrm{T}<45.0\ \mathrm{GeV}/c\ \ \text{for}\ \ 0.9<|y|<1.2\\
&6.5<p_\mathrm{T}<45.0\ \mathrm{GeV}/c\ \ \text{for}\ \ 1.2<|y|<1.6\\
&6.5<p_\mathrm{T}<30.0\ \mathrm{GeV}/c\ \ \text{for}\ \ 1.6<|y|<2.1\\
&5.5<p_\mathrm{T}<30.0\ \mathrm{GeV}/c\ \ \text{for}\ \ 2.1<|y|<2.4\quad ,
\end{aligned} \tag{2.2}$$

and for the $\psi(2\mathrm{S})$ cross sections is:

$$\begin{aligned}
&6.5<p_\mathrm{T}<30.0\ \mathrm{GeV}/c\ \ \text{for}\ \ |y|<1.2\\
&5.5<p_\mathrm{T}<30.0\ \mathrm{GeV}/c\ \ \text{for}\ \ 1.2<|y|<2.4\quad .
\end{aligned} \tag{2.3}$$

3 The CMS detector

A detailed description of the detector can be found elsewhere [13]. The central feature of the CMS apparatus, composed of a central barrel and two endcaps, is a 6 m diameter superconducting solenoid producing a 3.8 T magnetic field. Within the magnetic field volume are the silicon tracker, the crystal electromagnetic calorimeter, and the brass/scintillator hadron calorimeter.

The coordinate system adopted by CMS has the origin at the nominal collision point, the y axis pointing vertically upward, and the x axis pointing radially toward the centre of the LHC ring. The z axis points along the anti-clockwise beam direction defining a right-handed coordinate system. The polar angle θ is measured from the z axis. The pseudorapidity of a particle is defined as $\eta=-\ln[\tan(\theta/2)]$, which approaches the rapidity

JHEP02(2012)011

$y = 0.5 \ln[(E + cp_z)/(E - cp_z)]$ in the ultra-relativistic limit, where E and p_z are the particle's energy and longitudinal momentum.

Muons are detected in the pseudorapidity range $|\eta| < 2.4$ by three types of gas-based detectors embedded in the steel return yoke: drift tubes in the barrel, cathode strip chambers in the endcaps, and resistive plate chambers in both the barrel and endcaps.

The silicon tracker consists of the inner pixel-based detector followed by layers of microstrip detectors. The strong magnetic field and the good position resolution of the silicon tracker enable the transverse momentum of muons matched to reconstructed tracks to be measured with a resolution of $\sim 1.5\,\%$ for p_{T} smaller than $100\,\mathrm{GeV}/c$.

The first level (L1) of the CMS trigger system, composed of custom hardware processors, uses information from the calorimeters and muon detectors to select the most interesting events. The high level trigger (HLT) runs on a processor farm to reduce further the rate before data storage.

4 Data selection and event reconstruction

This analysis is based on a data sample collected in 2010 with the CMS detector, in pp collisions at a centre-of-mass energy of 7 TeV . The sample is selected to have consistent trigger requirements for the data used in the analysis and without overlap with the sample used in ref. [7]. It corresponds to a total integrated luminosity of $36.7 \pm 1.5\,\mathrm{pb}^{-1}$ [14]. During this data-taking period, there were on average 2.2 inelastic pp collisions per bunch crossing at the CMS interaction region.

The J/ψ and $\psi(2\mathrm{S})$ mesons are reconstructed in the $\mu^+\mu^-$ decay channel. This analysis is based on events selected by dimuon triggers that exploit advanced processing at the HLT level. Information from all three muon systems, as well as from the tracker, are used to make the trigger decision. Both muons are required to be consistent with a L1 muon signal, requiring at least two independent segments in the muon chambers, and to be matched to a track reconstructed in a region of interest defined by the L1 seed. No explicit requirement on the transverse momentum p_{T} is applied.

Simulated events are used to tune the selection criteria, check the agreement with data, compute the acceptance, and derive efficiency corrections, as well as for systematic studies. Prompt J/ψ and $\psi(2\mathrm{S})$ events are simulated using PYTHIA 6.422 [15], which generates events based on the leading-order colour-singlet and colour-octet mechanisms. Colour-octet states undergo a shower evolution. We use the NRQCD matrix element tuning obtained by fitting NRQCD calculations to CDF data [16, 17]. In the absence of consistent theoretical and experimental information about the J/ψ and $\psi(2\mathrm{S})$ polarizations, the dilepton decay distribution is assumed to be isotropic. Simulated events with b-hadron decays are also generated with PYTHIA, and the b hadrons are forced to decay inclusively into J/ψ and $\psi(2\mathrm{S})$ using the EvtGen package. Photon final-state radiation (FSR) is implemented using PHOTOS [18, 19].

The off-line event selection, only briefly summarized here, is very similar to the one used in ref. [7]. Muon candidates are reconstructed from the combination of muon-detector and silicon-tracker hits. The muons are required to pass the following criteria in the tracker:

JHEP02(2012)011

have at least 10 tracker hits, at least two of which are required to be in the pixel layers; have a χ^2 per degree of freedom smaller than 1.8; and pass within a cylinder of radius 3 cm and length 30 cm centred at the beam-spot centroid position and parallel to the beam line.

To select events with J/ψ or $\psi(2S)$ decays, muons with opposite charge are paired and their invariant mass is computed. The mass is required to be between 2.5 and 4.7 GeV/c^2. The two muon trajectories are refitted with a common vertex constraint, and events are retained if the χ^2 probability of the fit is larger than 1%. If more than one muon pair is found in the event, the one with the largest vertex χ^2 probability is retained.

The dimuon L1 triggers include a veto, whose specific criteria depend on the type of muon chamber and the region of the detector: this rejects muon signals whose spatial separation in the muon stations is too small, in order to avoid spurious dimuon signatures from a single muon. As a consequence, the dimuon sample is split in two, depending on the signed difference in azimuthal angle ($\Delta\phi$) between the positively and the negatively charged muons. Muons that bend towards each other in the magnetic field are called type-C ("convergent") dimuons, while muons that bend away from each other are type-D ("divergent") dimuons.

Dimuons of type D are much less affected by the trigger veto, while dimuons of type C may cross at the muon stations. This causes sizeable correlations between the two muon detection efficiencies, and this effect is larger in the forward region. Therefore, in addition to the above requirements, all type-C dimuons are rejected for the inclusive cross section measurements. This corresponds to a 48% reduction in the yield. For the non-prompt fraction determination (which is largely efficiency independent), type-C dimuons are only rejected in the high dimuon rapidity region $1.6 < |y| < 2.4$.

The momentum measurement of charged tracks in the CMS detector has systematic uncertainties that are due to imperfect knowledge of the magnetic field, modelling of the detector material, and sub-detector misalignment. These effects can shift and change the width of the mass peaks of dimuon resonances. In addition to calibrations already applied to the data [20–22], residual effects are determined by studying the dependence of the reconstructed dimuon peak shapes on the muon kinematics, as was done in ref. [7].

5 Inclusive yield determination

Two methods are used to extract the inclusive yields from the $\mu^+\mu^-$ invariant mass distribution, either fitting the J/ψ peak alone in a restricted mass window, or fitting the combined J/ψ and $\psi(2S)$ distribution. Yields are derived using an extended unbinned maximum-likelihood method.

In both types of fits, the sum of a Gaussian and a Crystal Ball [23] function is used for the description of the signals, simultaneously taking into account FSR and rapidity-dependent resolution variations. In the J/ψ-only fits, an exponential function is used to describe the background. Figure 1 (top) shows an example of a fitted mass distribution.

In the second type of fits, the two mass peaks and the background are fitted simultaneously. For both the J/ψ and $\psi(2S)$ signal peaks the probability density function (pdf) defined before, i.e. the sum of a Gaussian and a Crystal Ball function, is used, with the

JHEP02(2012)011

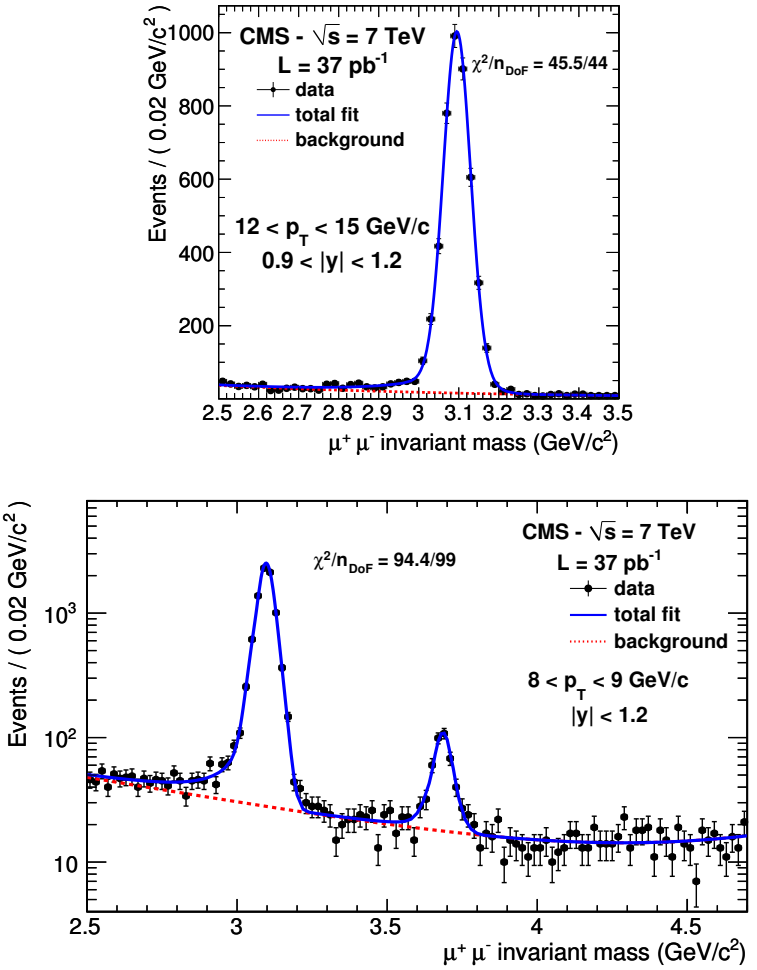

Figure 1. Top: the $\mu^+\mu^-$ invariant mass distribution in the J/ψ region and the result of the fit for the bin: $0.9 < |y| < 1.2$, $12 < p_{\mathrm{T}} < 15$ GeV/c. Bottom: J/ψ and $\psi(2\mathrm{S})$ mass distribution fit for the bin: $|y| < 1.2$, $8 < p_{\mathrm{T}} < 9$ GeV/c. The solid and dashed lines represent the total fits and their background components, respectively.

following constraints on the parameters: the ratio of the central values of the two masses is fixed to the world average value [24]; the widths, scaled by the nominal mass values, are constrained to be the same, and the parameters describing the asymmetric tail of the Crystal Ball function (α and n) are constrained to be equal. The background is modelled by two exponentials. Figure 1 (bottom) shows an example of a fitted mass distribution. The ranges of values obtained for the J/ψ width (expressed as the weighted mean of the Gaussian and Crystal Ball widths), α and n are reported in table 1.

The systematic uncertainties on the mass distribution fits are estimated by changing the analytical form of the signal and background pdf hypotheses (a single Crystal Ball function is used for the signal and polynomial pdfs for the background) in the two types of fits. The largest variation in the yield of each fit is taken as the systematic uncertainty.

JHEP02(2012)011

$\|y\|$ range	Mass resolution (MeV/c^2)	α	n
$0.0 - 1.2$	20-38	0.8-2.1	4-8
$1.2 - 1.6$	39-49	0.9-1.6	5-9
$1.6 - 2.4$	58-71	1.0-2.5	4-10

Table 1. Mass resolution and Crystal Ball parameters ranges for J/ψ, as obtained from J/ψ and ψ(2S) fits.

6 Acceptance and efficiency

As discussed in section 1, measurements will be presented using two different approaches. In the first approach, the observed number of J/ψ events is corrected for the detector acceptance and reconstruction efficiency in every bin in which the cross section is measured. As the acceptance is strongly dependent on the assumed polarization of the charmonium state, in the second approach we provide measurements exclusively within the CMS detector acceptance, where only detector efficiency corrections are made and without any polarization-related uncertainties.

6.1 Acceptance

The acceptance reflects the geometrical coverage of the CMS detector and the kinematic reach of the muon trigger and reconstruction, constrained by the amount of material in front of the muon detectors and by the track curvature in the magnetic field.

In the simulation, both muons are required to be within the geometric acceptance of the muon detectors. A single muon is defined as detectable if it satisfies the following requirements at generator level:

$$\begin{aligned} p_{\mathrm{T}}^{\mu} &> 4.0 \ \text{GeV}/c \quad \text{for} \quad |\eta^{\mu}| < 1.2 \\ p_{\mathrm{T}}^{\mu} &> 3.3 \ \text{GeV}/c \quad \text{for} \quad 1.2 < |\eta^{\mu}| < 2.4 \quad . \end{aligned} \tag{6.1}$$

The J/ψ acceptance A is defined as the fraction of $J/\psi \to \mu^+\mu^-$ decays in which both muons are detectable, as a function of the generated dimuon transverse momentum p_{T} and rapidity y,

$$A(p_{\mathrm{T}}, y; \lambda_\theta) = \frac{N_{\mathrm{det}}(p_{\mathrm{T}}, y; \lambda_\theta)}{N_{\mathrm{gen}}(p_{\mathrm{T}}, y; \lambda_\theta)} \quad , \tag{6.2}$$

where N_{det} is the number of detectable J/ψ events in a given (p_{T}, y) bin, and N_{gen} is the corresponding total number of generated J/ψ events in the Monte Carlo (MC) simulation. An analogous definition holds for ψ(2S). The parameter λ_θ reflects the fact that the acceptance is computed for various polarization scenarios, which lead to different muon spectra in the laboratory frame.

For the acceptance calculation, a dedicated sample of generated events is used, with no restrictions on the phase space. The large number of simulated events allows a much smaller bin size for determining A with respect to that used for the cross section determination in data.

To study the effect of J/ψ and ψ(2S) polarization on the acceptance, these events are reweighted depending on the values of the polar and azimuthal angles as computed in two

JHEP02(2012)011

different frames (helicity and Collins-Soper [25]). The angular distribution for the decay of a $J = 1$ state into fermions is used, which is a function of three independent parameters λ_θ, λ_ϕ, and $\lambda_{\theta\phi}$:

$$W(\cos\theta, \phi) = \frac{3}{2(3+\lambda_\theta)} \cdot (1 + \lambda_\theta \cos^2\theta + \lambda_\phi \sin^2\theta \cos 2\phi + \lambda_{\theta\phi} \sin 2\theta \cos\phi) \quad . \tag{6.3}$$

The choice of zero for all λ parameters corresponds to an unpolarized decay, while $\lambda_\theta = -1$ and $\lambda_\theta = +1$ correspond to fully longitudinal and fully transverse polarizations, respectively.

By default, the prompt J/ψ and $\psi(2S)$ are assumed to be unpolarized, while the non-prompt mesons are assumed to be polarized as generated by EvtGen and corrected to match recent measurements, as mentioned in the Introduction. Typical changes of the measured cross sections when using alternative polarization scenarios are provided in section 9.

Several sources of systematic uncertainty on the acceptance have been investigated:

- *Kinematic spectra.* Different p_T and y spectra of the generated J/ψ and $\psi(2S)$ might produce different acceptances, as the acceptance is defined by single-muon criteria. Spectra from theoretical predictions presented in section 9 have been used to recompute the acceptance, and the difference from that obtained with the PYTHIA spectrum has been taken as a systematic uncertainty.

- *Final-state radiation.* The generated dimuon momentum may differ from the J/ψ and $\psi(2S)$ momentum, because of FSR. The difference between the acceptance computed using the J/ψ or $\psi(2S)$ rapidity and p_T, before and after FSR emission in eq. (6.2) is taken as a systematic uncertainty.

- B *polarization.* The J/ψ and $\psi(2S)$ mesons produced in b-hadron decays have a different acceptance with respect to the prompt ones. The corresponding systematic uncertainty is evaluated by taking the difference of the default choice (corrected to match the experimental results of ref. [12]) with respect to the one predicted by EvtGen.

- p_T *calibration.* The muon transverse momenta in data have been calibrated as described in ref. [7]. A difference in the momentum resolution between data and simulated events would also give a systematic uncertainty on the acceptance. The acceptance has been computed with simulated muon momenta smeared according to the resolution measured with data [26]. The uncertainty on the measured resolution was used to apply an additional smearing on the simulated momenta; the acceptance has been recalculated and the shift taken as a systematic uncertainty.

6.2 Muon efficiency

The single-muon efficiency is measured from data for muons in the acceptance, as described in refs. [27, 28], and is based on the *tag-and-probe* (T&P) method. For this purpose,

JHEP02(2012)011

independent sets of triggers are used for which online requirements either on the muon or the tracker tracks are not applied, thus yielding samples which are unbiased with respect to the corresponding selections.

The combined trigger and offline reconstruction efficiency for a single muon is defined as:

$$\epsilon(\mu) = \epsilon_{\text{trig | off}} \cdot \epsilon_{\text{off | ID}} \cdot \epsilon_{\text{ID | track}} \cdot \epsilon_{\text{track}}, \tag{6.4}$$

where ϵ_{track} is the offline tracking efficiency, $\epsilon_{\text{ID | track}}$ refers to the muon identification in the muon systems for a tracker-reconstructed muon, $\epsilon_{\text{off | ID}}$ refers to the specific quality requirements applied to reconstructed muons, and $\epsilon_{\text{trig | off}}$ is the probability for an offline reconstructed muon to have also fired the trigger.

The muon identification and trigger efficiencies ($\epsilon_{\text{trig | off}}$, $\epsilon_{\text{off | ID}}$ and $\epsilon_{\text{ID | track}}$) have the strongest p_{T}^{μ} and $|\eta^{\mu}|$ dependence and are determined in 15 bins of p_{T}^{μ} ($3.3 < p_{\text{T}}^{\mu} < 50\,\text{GeV}/c$) and 14 bins of $|\eta^{\mu}|$ ($0 < |\eta^{\mu}| < 2.4$), allowing an adequate description of the turn-on efficiency curves. Since the tracking efficiency is almost constant for this momentum and rapidity range, broader bins are used.

The efficiency to detect a dimuon event is expressed as:

$$\epsilon(\mu^+\mu^-) = \epsilon(\mu^+) \cdot \epsilon(\mu^-) \cdot \rho \cdot \epsilon_{\text{vertex}}, \tag{6.5}$$

where $\epsilon(\mu^+)$ and $\epsilon(\mu^-)$ are the single-muon efficiencies, and ϵ_{vertex} is the efficiency of the vertex χ^2 requirement, calculated from the data by determining the yields in regions of large p_{T} and $|y|$ by alternatively applying and not applying this requirement. The ρ factor, defined by eq. (6.5), represents a correction to the efficiency factorization hypothesis: it accounts for the finite size of the $(p_{\text{T}}^{\mu}, \eta^{\mu})$ bins and, more importantly, for the possible bias introduced by the T&P measurement, due to correlation effects as discussed in section 4. In order to determine ρ, the efficiencies have also been evaluated using T&P techniques on simulated events and their product has been compared with the true dimuon efficiency. Except for some bins at high p_{T}, the values are found to satisfy $|1 - \rho| < 10\%$.

For the acceptance-corrected cross section results, the acceptance and efficiencies are combined into a single factor, which is computed for each (p_{T}, y) bin and is defined as:

$$\left\langle \frac{1}{A \cdot \epsilon} \right\rangle_{\text{bin}} \equiv \frac{1}{N_{\text{event}}} \sum_{k=1}^{N_{\text{event}}} \frac{1}{A_k \cdot \epsilon_k(\mu^+\mu^-)}, \tag{6.6}$$

where the average is taken over the data events in each bin, using the "fine-grained" bins of the acceptance and the event-by-event efficiency obtained from the single-muon efficiencies using eq. (6.5). Values of $\langle \frac{1}{A \cdot \epsilon} \rangle_{\text{bin}}$ for the J/ψ bins used in the analysis are shown in figure 2.

Similarly, for the results which are not corrected for acceptance, the efficiency factor is determined as:

$$\left\langle \frac{1}{\epsilon} \right\rangle_{\text{bin}} \equiv \frac{1}{N_{\text{event}}} \sum_{k=1}^{N_{\text{event}}} \frac{1}{\epsilon_k(\mu^+\mu^-)}. \tag{6.7}$$

Two sources of systematic uncertainty in the efficiency are considered:

JHEP02(2012)011

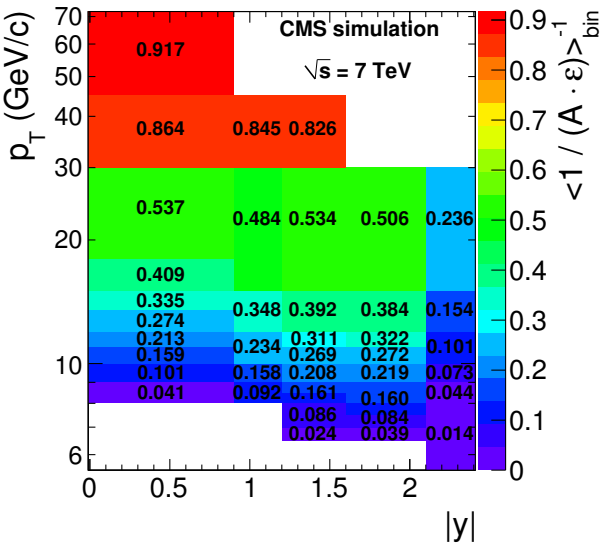

Figure 2. Averaged acceptance-efficiency correction factor for J/ψ detection as a function of p_{T} and $|y|$ in the bins used in the measurement. Related uncertainties are listed in table 2.

- The uncertainties on the measured muon efficiencies propagate as systematic errors on the cross section measurement through the correction factor $\langle \frac{1}{A \cdot \epsilon} \rangle_{\mathrm{bin}}$ (or $\langle \frac{1}{\epsilon} \rangle_{\mathrm{bin}}$). The effect has been estimated on a statistical basis in each bin by performing Monte Carlo pseudo-experiments, in which the muon efficiencies were varied randomly according to a probability density built by joining the left and the right side of two Gaussians with different widths, in order to allow for asymmetric errors. The r.m.s. of these correction factors in each bin has been taken as the systematic uncertainty associated with the single-muon efficiency.

- The full difference $|1 - \rho|$ in each bin is taken as a systematic uncertainty due to the efficiency correlation.

7 Inclusive cross section determination

The inclusive double-differential cross section is obtained using eq. (2.1).

Figure 3 shows the measured (fully corrected) J/ψ inclusive cross section as a function of p_{T} for the various rapidity bins. They are compared with our previous results published in ref. [7], which are statistically independent and remain of interest since they partially overlap with the present results and cover a lower p_{T} range. A good agreement is observed. In this figure, as well as in the cross section plots of section 9, multiplicative factors — appearing as additive offsets on the log scale — are used to achieve a convenient graphical separation of the measurements from different rapidity bins.

JHEP02(2012)011

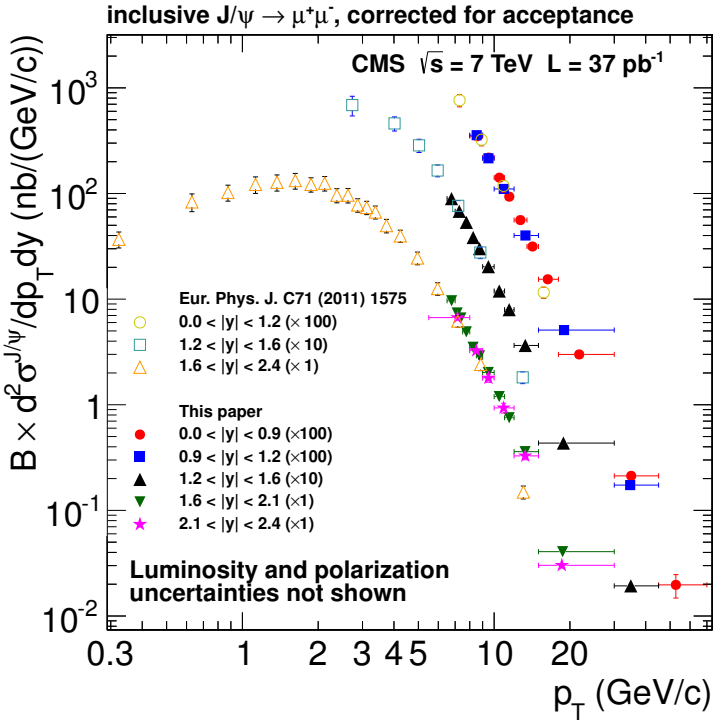

Figure 3. Measured differential cross section for J/ψ inclusive production as a function of p_{T} for five rapidity bins, fully corrected for acceptance and efficiency. Also plotted are the results published in ref. [7], which extend to a lower p_{T} range. The error bars on data points include all the statistical and systematic contributions except luminosity and polarization. The measurements have been offset by the numerical values given in the legend for easier viewing.

8 Prompt and non-prompt fractions

To estimate the J/ψ fraction from b-hadron decays, a two-dimensional fit is performed, in which the pdfs and fit procedure are the same as those described in ref. [7]. The variables used for the two-dimensional fits are the dimuon invariant mass and the "pseudo proper decay length" $\ell_{J/\psi}$, defined as the most probable value of the transverse distance between the dimuon vertex and the primary vertex, corrected by the transverse Lorentz boost of the J/ψ. As in ref. [7], the primary vertex is chosen as the one closest to the dimuon vertex in the z direction.

The resolution of the pseudo proper decay length is described by a function depending on an event-by-event uncertainty determined from the covariance matrices of the primary and secondary vertex fits. The uncertainty is used as the r.m.s. of the resolution Gaussian function that describes the core of the resolution, while a second Gaussian function with a small relative normalization (usually $< 1\%$) parametrizes the effect of incorrect primary vertex assignments.

The pdf $F(\ell_{J/\psi}, m_{\mu\mu}, \sigma_\ell)$ for the J/ψ is then:

$$\begin{aligned} F(\ell_{J/\psi}, m_{\mu\mu}, \sigma_\ell) = {} & f_{\mathrm{Sig}} \cdot D_{\mathrm{Sig}}(\sigma_\ell) \cdot F_{\mathrm{Sig}}(\ell_{J/\psi}, \sigma_\ell) \cdot M_{\mathrm{Sig}}(m_{\mu\mu}) + \\ & (1 - f_{\mathrm{Sig}}) \cdot D_{\mathrm{Bkg}}(\sigma_\ell) \cdot F_{\mathrm{Bkg}}(\ell_{J/\psi}, \sigma_\ell) \cdot M_{\mathrm{Bkg}}(m_{\mu\mu}), \end{aligned} \tag{8.1}$$

JHEP02(2012)011

where:

$$F_k(\ell_{J/\psi}, \sigma_\ell) = \sum_{i=1}^{2} F_k^{\rm true}(\ell'_{J/\psi}) \otimes R_i(\ell_{J/\psi} - \ell'_{J/\psi}|\mu, s_i\sigma_\ell) \tag{8.2}$$

and $k = \{\text{Sig, Bkg}\}$. In the equations above:

- $M_{\rm Sig}(m_{\mu\mu})$ and $M_{\rm Bkg}(m_{\mu\mu})$ are the mass pdfs determined for the signal and background in section 5, and $f_{\rm Sig}$ is the fraction of signal events in the entire range of the fit;

- $F_{\rm Sig}^{\rm true}(\ell_{J/\psi})$ and $F_{\rm Bkg}^{\rm true}(\ell_{J/\psi})$ are the functional forms describing the $\ell_{J/\psi}$ distribution for the signal and background, respectively. The signal part is given by the sum of prompt and non-prompt components: $F_{\rm Sig}^{\rm true}(\ell_{J/\psi}) = f_b \cdot f_b(\ell_{J/\psi}) + (1 - f_b) \cdot F_p(\ell_{J/\psi})$, where f_b is the fraction of J/ψ from b-hadron decays, and $F_p(\ell_{J/\psi})$ and $f_b(\ell_{J/\psi})$ are the $\ell_{J/\psi}$ distributions for prompt and non-prompt J/ψ, respectively. The $\ell_{J/\psi}$ pdfs for prompt signal and background are the same as in ref. [7]. The non-prompt lifetime function is described by an exponential decay of the b hadron, with a Gaussian smearing function that accounts for the difference between the measured pseudo proper decay length and the proper decay length of the b hadron;

- σ_ℓ is the per-event uncertainty of the decay length and $D_{\rm Sig}(\sigma_\ell)$ and $D_{\rm Bkg}(\sigma_\ell)$ are its distributions separately for signal and background [29]. They are obtained from the signal region of the invariant mass distribution, after a sideband subtraction, and the sideband regions, respectively;

- R_1 and R_2 represent the core and tail decay-length resolution Gaussian functions: μ is their common mean and s_i represent scale factors for the per-event uncertainty, which are both left free in the fit to account for initial assumptions on the uncertainties of track parameters. These functions are convolved with $F_k^{\rm true}(\ell_{J/\psi})$ to obtain the observed $F_k(\ell_{J/\psi})$ distributions, including the experimental resolution ($k = \{\text{Sig, Bkg}\}$).

The background is fitted using the events in mass sidebands and the result is used to fix lifetime parameters of the overall fit in the entire mass region. The mass sideband region is defined as [2.50, 2.85] and [3.25, 3.35] GeV/c^2.

For the determination of the ψ(2S) non-prompt fraction, the quantity $\ell_{\psi(2S)}$, defined as for the J/ψ case, is computed. In order to constrain the fit and avoid problems due to limited statistical accuracy, the J/ψ and ψ(2S) samples are fitted simultaneously using the same binning as for the ψ(2S) cross section determination. The lifetime resolution functions R_1 and R_2 are constrained to be described by the same parameters (mean value and scale factors) and the backgrounds to have the same fractions of long-lived components.

The invariant mass sideband regions used for the determination of the background parameters are defined as above for the J/ψ, and as [3.35, 3.45] and [3.85, 4.20] GeV/c^2 for the ψ(2S).

Figure 4 shows two examples of the $\ell_{J/\psi}$ and $\ell_{\psi(2S)}$ distributions with projections of two-dimensional fits on these dimensions, as well as the prompt and non-prompt components

JHEP02(2012)011

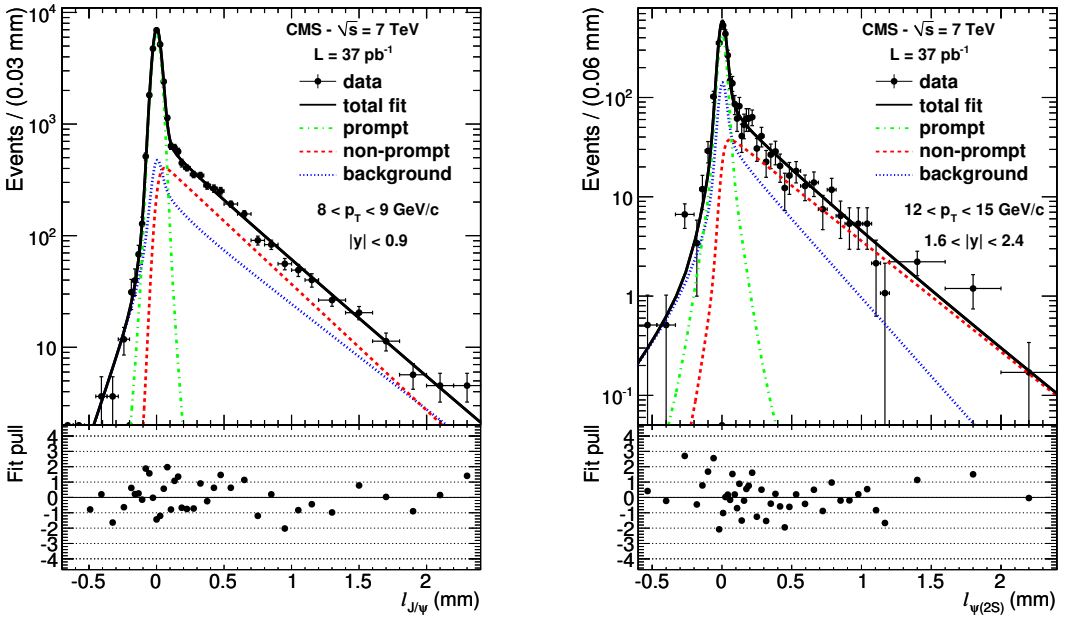

Figure 4. Left: projection of a J/ψ two-dimensional fit on the $\ell_{J/\psi}$ dimension in the bin $|y| < 0.9$, $8 < p_{\mathrm{T}} < 9\,\mathrm{GeV}/c$ and in the whole mass region [2.50, 3.35] GeV/c^2. Right: projection of a J/ψ-$\psi(2\mathrm{S})$ two-dimensional fit on the $\ell_{\psi(2\mathrm{S})}$ dimension in the bin: $1.6 < |y| < 2.4$, $12 < p_{\mathrm{T}} < 15\,\mathrm{GeV}/c$, in the $\psi(2\mathrm{S})$ mass region [3.35, 4.20] GeV/c^2. The solid lines represent the total fits; the prompt, non-prompt and background components are also shown using green dash-dotted, red dashed and blue dotted lines, respectively. The fit pull plots show no systematic structures.

obtained as described above. The lower plots in figure 4 give the pull distributions from the fits, and show no systematic structure.

Several sources of systematic uncertainty have been addressed, using mostly the same procedures as in ref. [7]. The main additional systematic effect comes from attempting to choose the correct primary vertex of the interaction in the presence of pile-up. The sources of systematic uncertainty include the following:

- *Primary vertex assignment.* In order to estimate the possible effect of pile-up on the primary vertex estimation, the primary vertex associated to the dimuon is chosen as the one with the largest track $\sum {p_{\mathrm{T}}}^2$, instead of the one closest in z to the dimuon vertex. The difference between the fitted non-prompt fractions in these two approaches is taken as the systematic uncertainty.

- *Residual misalignment in the tracker.* The effect of uncertainties in the measured misalignment of the tracker modules is estimated by reconstructing the data using different sets of alignment constants. The largest difference in the fit results with respect to the nominal case is taken as the systematic uncertainty.

JHEP02(2012)011

- *b-hadron lifetime model.* An alternative fit method is used, namely the b-hadron lifetime model used in ref. [7], which is based on MC templates; the difference in the fitted non-prompt fraction is taken as the systematic uncertainty.

- *Background fits.* The effect of a $\pm 100\,\mathrm{MeV}/c^2$ variation in the lower limit of the low-mass side (upper limit of the high-mass side) of the J/ψ ($\psi(2S)$) sideband boundaries is taken as the systematic uncertainty.

- *Resolution model.* The nominal (double-Gaussian) model for the pseudo proper decay length per-event resolution is compared with a model using a single-Gaussian shape. The difference is taken as the systematic uncertainty.

- *Different prompt and non-prompt efficiencies.* The MC simulation predicts slight differences between the prompt and non-prompt J/ψ and $\psi(2S)$ efficiencies, mostly because of the different track densities from fragmentation products around the muons. These are taken into account; the relative difference is propagated to the non-prompt fraction, and taken as the systematic uncertainty.

Non-prompt fraction results are given in section 9 and a summary of all the systematic uncertainties is given in tables 2 and 3 for the J/ψ and $\psi(2S)$, respectively.

9 Results

The prompt and non-prompt double differential cross sections for the two charmonium states are obtained by multiplying the measured inclusive cross sections with the fraction of prompt and non-prompt events, respectively. In addition the cross section ratio of the two charmonium states is calculated.

Statistical uncertainties and contributions from the investigated sources to the total systematic uncertainties on these cross sections are summarized in tables 2 and 3. The largest uncertainties are due to the efficiency correlations; FSR estimation has a sizeable effect only in bins close to the edges of the acceptance.

9.1 Prompt and non-prompt cross sections corrected for acceptance

Figures 5 and 6 show the measured prompt and non-prompt cross sections for the J/ψ and the $\psi(2S)$ as a function of p_T, for the various rapidity bins and corrected for detector acceptance. They are compared with theoretical predictions from NRQCD [3] and from FONLL [5, 6] for the prompt and non-prompt cases, respectively. Numerical values are also reported in ref. [30]. Integrated cross sections in the p_T and rapidity ranges defined by eqs. (2.2)–(2.3) are also reported. They are computed to be:

$$\begin{aligned}\mathcal{B}(J/\psi \to \mu^+\mu^-) \cdot \sigma(\mathrm{pp} \to \text{prompt } J/\psi) &= 54.5 \pm 0.3 \pm 2.3 \pm 2.2 \text{ nb} \quad , \\ \mathcal{B}(J/\psi \to \mu^+\mu^-) \cdot \sigma(\mathrm{pp} \to \mathrm{b}X \to J/\psi X) &= 20.2 \pm 0.2 \pm 0.8 \pm 0.8 \text{ nb}\end{aligned}$$

for prompt and non-prompt J/ψ production, respectively, and:

$$\begin{aligned}\mathcal{B}(\psi(2S) \to \mu^+\mu^-) \cdot \sigma(\mathrm{pp} \to \text{prompt } \psi(2S)) &= 3.53 \pm 0.26 \pm 0.32 \pm 0.14 \text{ nb} \quad , \\ \mathcal{B}(\psi(2S) \to \mu^+\mu^-) \cdot \sigma(\mathrm{pp} \to \mathrm{b}X \to \psi(2S)X) &= 1.47 \pm 0.12 \pm 0.13 \pm 0.06 \text{ nb}\end{aligned}$$

JHEP02(2012)011

$\lvert y\rvert$ range		$0-0.9$	$0.9-1.2$	$1.2-1.6$	$1.6-2.1$	$2.1-2.4$
Quantity affected	Source	Relative uncertainty (in %)				
All cross sections						
$m_{\mu\mu}$ fits	Statistical	$1.2-8.9$	$1.5-7.1$	$1.6-8.4$	$1.2-3.2$	$2.3-3.9$
$\ell_{J/\psi}$ fits	Statistical	$1.0-5.9$	$1.4-4.7$	$1.4-7.6$	$2.1-8.3$	$4.4-7.1$
Efficiency	Single-muon efficiency	$0.3-0.9$	$0.2-1.6$	$0.1-1.4$	$0.2-1.0$	$0.6-1.4$
	ρ factor	$1.9-23.2$	$1.2-7.6$	$0.7-5.7$	$0.8-5.4$	$3.7-6.8$
Yields	Fit functions	$0.6-3.4$	$0.4-2.8$	$0.5-2.8$	$0.8-2.2$	$1.0-4.2$
Luminosity	Luminosity	4.0	4.0	4.0	4.0	4.0
Non-prompt fraction	Tracker misalignment	$0.1-2.1$	$0.1-0.8$	$0.0-1.5$	$0.2-3.2$	$0.2-5.1$
	b-lifetime model	$0.1-3.0$	$0.1-3.4$	$0.1-3.7$	$0.2-2.6$	$0.2-6.6$
	Vertex estimation	$0.1-0.7$	$0.7-3.0$	$0.4-3.7$	$1.5-4.6$	$2.3-5.0$
	Background fit	$0.0-0.2$	$0.1-1.4$	$0.1-1.0$	$0.0-2.5$	$0.1-1.2$
	Resolution model	$0.2-3.5$	$0.0-4.2$	$0.8-3.5$	$1.1-5.0$	$1.1-4.4$
	Efficiency	$0.4-2.1$	$0.9-3.3$	$0.5-9.9$	$0.3-3.3$	$1.6-10.5$
Only acceptance-corrected cross sections						
Acceptance	FSR	$0.0-1.5$	$0.0-2.5$	$0.0-4.2$	$0.7-8.0$	$0.5-3.5$
	p_{T} calibration	$0.0-0.6$	$0.0-0.6$	$0.0-0.8$	$0.1-0.6$	$0.0-0.8$
	Kinematic spectra	$0.0-0.3$	$0.0-0.7$	$0.0-0.7$	$0.7-3.8$	$0.4-5.3$
	B polarization	$0.0-0.5$	$0.0-0.4$	$0.0-0.5$	$0.1-0.8$	$0.3-1.3$

Table 2. Summary of the relative statistical and systematic uncertainties on the non-prompt J/ψ cross section (in %). The variation over the different p_{T} bins is given for the five rapidity regions. Uncertainties on the prompt cross section are identical, with the exception of the non-prompt fraction, where they must be regarded as relative to $(1-f_b)$ rather than to f_b. Acceptance uncertainties on the FSR are given, excluding the lowest-p_{T} bin in every rapidity region, where it can be as large as 19% because of acceptance edge effects.

for prompt and non-prompt $\psi(2\mathrm{S})$ production, respectively. In the equations above the first uncertainty is statistical, the second systematic and the third coming from the luminosity measurement.

The NRQCD prediction includes non-prompt production in the J/ψ case caused by feed-down decays from heavier charmonia, and can therefore be directly compared with the data. Good agreement is found in both the J/ψ and the $\psi(2\mathrm{S})$ cases. For non-prompt production there is an overall shift of the measurements with respect to the FONLL predictions, although within the quoted uncertainty. In general, for both states, the observed differential cross sections seem to fall more rapidly than the FONLL prediction at high p_{T}, and this effect is more evident for the J/ψ because of the higher p_{T} reach.

The NRQCD theoretical uncertainties include those on the feed-down contributions and on the colour-octet, long-distance matrix elements determined from fits to the Tevatron data. The FONLL theoretical errors include uncertainties on $\mathcal{B}(\mathrm{B}\to J/\psi\ X)$ and $\mathcal{B}(\mathrm{B}\to\psi(2\mathrm{S})X)$, renormalization and factorization scales, b-quark and c-quark masses, parton distribution functions, and b-fragmentation parameters.

JHEP02(2012)011

$\|y\|$ range		$0 - 1.2$	$1.2 - 1.6$	$1.6 - 2.4$
Quantity affected	Source	Relative uncertainty (in %)		
All cross sections				
$m_{\mu\mu}$ fits	Statistical	$5.6 - 14.8$	$7.5 - 31.7$	$7.3 - 24.1$
$\ell_{\psi(2S)}$ fits	Statistical	$4.3 - 12.7$	$5.9 - 38.0$	$9.1 - 26.4$
Efficiency	Single-muon efficiency	$0.1 - 0.5$	$0.1 - 0.6$	$0.2 - 0.9$
	ρ factor	$0.7 - 13.1$	$2.1 - 6.6$	$2.3 - 9.8$
Yields	Fit functions	$1.2 - 3.7$	$0.6 - 12.1$	$3.1 - 10.0$
Luminosity	Luminosity	4.0	4.0	4.0
Non-prompt fraction	Tracker misalignment	$0.3 - 2.6$	$1.5 - 7.1$	$1.8 - 11.1$
	b-lifetime model	$0.0 - 2.5$	$0.4 - 7.6$	$0.0 - 2.9$
	Vertex estimation	$0.0 - 1.7$	$0.2 - 3.5$	$1.2 - 4.2$
	Background fit	$1.0 - 6.8$	$2.2 - 10.0$	$2.5 - 15.3$
	Resolution model	$0.5 - 3.5$	$0.1 - 4.6$	$0.9 - 24.9$
	Efficiency	$0.5 - 7.8$	$0.9 - 6.3$	$0.5 - 13.8$
Only acceptance-corrected cross sections				
Acceptance	FSR	$0.0 - 3.9$	$0.5 - 3.4$	$0.3 - 4.1$
	p_{T} calibration	$0.2 - 0.5$	$0.3 - 0.5$	$0.3 - 0.5$
	Kinematic spectra	$0.1 - 1.2$	$0.0 - 0.9$	$0.7 - 2.0$
	B polarization	$0.1 - 0.8$	$0.0 - 0.6$	$0.2 - 1.7$

Table 3. Summary of the relative statistical and systematic uncertainties in the non-prompt $\psi(2S)$ cross section (in %). The variation over the different p_{T} bins is given for the three rapidity regions. Uncertainties on the prompt cross section are identical, with the exception of the non-prompt fraction, where they must be regarded as relative to $(1 - f_b)$ rather than to f_b. Acceptance uncertainties on the FSR are given excluding the lowest-p_{T} bin in every rapidity region, where it can be as large as 29% because of acceptance edge effects.

However, uncertainties on the B $\to$ charmonium decay spectrum were not included in the original FONLL prediction. To estimate those, we make use of the EvtGen MC generator, which describes B $\to$ charmonium decays using a sum of many exclusive modes. We split the decay modes into two categories, "high-Q" and "low-Q", if the value of Q in the decay is respectively greater than or less than $1.2\,\mathrm{GeV}/c^2$, where $Q = m_{\mathrm{B}} - \sum_i m_i$ and the index i runs over the B decay products. As low-Q (high-Q) modes yield charmonia with smaller (larger) momentum in the B rest frame, they populate different regions of the B-decay spectrum. Two sets of non-prompt charmonium MC events are generated according to the following criteria. In the first, each high-Q mode branching fraction is increased by its world-average uncertainty [24] or by 100% of its value if the branching fraction is not measured. Low-Q mode branching fractions are decreased by a similar amount, rescaling the sum to unity after this procedure. In the second, the treatment of the high- and low-Q modes is interchanged. The maximum difference in the resulting spectra in the two cases is added to the theoretical FONLL uncertainty.

To investigate the effect of the assumed J/ψ and $\psi(2S)$ polarizations on the prompt cross section, the acceptance is recomputed for four extreme polarization scenarios corre-

sponding to fully longitudinal or fully transverse polarization in the helicity and Collins-Soper frames [25]. This produces relative cross section shifts across the entire kinematic range of up to 18-20% (20-25%) for the J/ψ (ψ(2S)) in the helicity frame, and 6-15% for both states in the Collins-Soper frame. Detailed results can be found in ref. [30].

9.2 Prompt and non-prompt cross sections uncorrected for acceptance

As discussed previously, since the polarization effects are large compared to the measurement uncertainties, cross section values are also reported that are restricted to the CMS muon acceptance region, to allow future measurements of the J/ψ and ψ(2S) polarization to be exploited.

Figures 7 and 8 show the measured prompt and non-prompt cross sections for the J/ψ and the ψ(2S) as a function of p_{T} for the various rapidity bins and uncorrected for detector acceptance. Numerical values can be found in ref. [30].

Integrated cross sections in the p_{T} and rapidity ranges defined by eqs. (2.2)–(2.3) are also reported uncorrected for acceptance, i.e. for both muons satisfying the conditions defined in eq. (6.1). They are computed to be:

$$\begin{aligned} \mathcal{B}(J/\psi \to \mu^+\mu^-) \cdot \sigma(\mathrm{pp} \to \text{prompt } J/\psi) &= 9.83 \pm 0.03 \pm 0.38 \pm 0.39 \text{ nb} \quad , \\ \mathcal{B}(J/\psi \to \mu^+\mu^-) \cdot \sigma(\mathrm{pp} \to \mathrm{b}X \to J/\psi X) &= 4.67 \pm 0.02 \pm 0.17 \pm 0.19 \text{ nb} \end{aligned}$$

for prompt and non-prompt J/ψ production, respectively, and:

$$\begin{aligned} \mathcal{B}(\psi(2\mathrm{S}) \to \mu^+\mu^-) \cdot \sigma(\mathrm{pp} \to \text{prompt } \psi(2\mathrm{S})) &= 0.410 \pm 0.009 \pm 0.023 \pm 0.016 \text{ nb} \quad , \\ \mathcal{B}(\psi(2\mathrm{S}) \to \mu^+\mu^-) \cdot \sigma(\mathrm{pp} \to \mathrm{b}X \to \psi(2\mathrm{S})X) &= 0.235 \pm 0.006 \pm 0.013 \pm 0.009 \text{ nb} \end{aligned}$$

for prompt and non-prompt ψ(2S) production, respectively. In the equations above the first uncertainty is statistical, the second systematic and the third coming from the luminosity measurement.

9.3 Non-prompt fractions

The measured non-prompt fractions for J/ψ and ψ(2S) mesons, extracted as described in section 8 and uncorrected for acceptance, are reported in ref. [30] and shown in figure 9. The uncertainties shown are statistical and systematic, and the measured values are plotted as a function of p_{T} in three rapidity ranges. In agreement with previous measurements [4, 7], we observe similar sizes of non-prompt fractions for J/ψ and ψ(2S), and an increasing trend with p_{T}. Acceptance corrections do not induce significant changes in the non-prompt fractions within their uncertainties.

9.4 Cross section ratio

Most of the systematic uncertainties on the acceptances and efficiencies listed in tables 2 and 3, as well as the luminosity uncertainty, cancel partially or fully in the ratio of the ψ(2S) to J/ψ cross sections. For this reason we also present the ratio of the two differential

JHEP02(2012)011

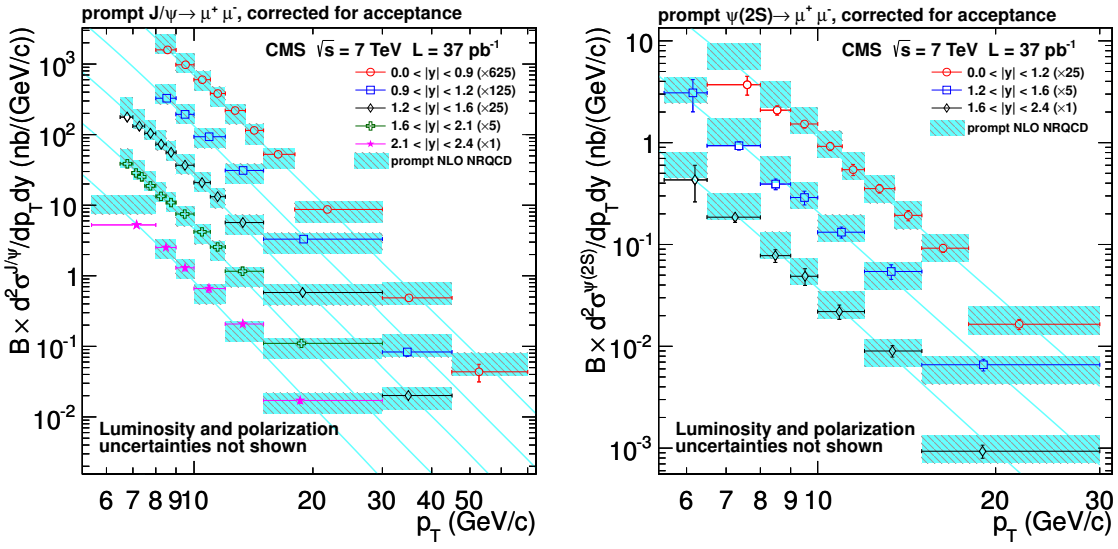

Figure 5. Measured differential cross section for prompt J/ψ and ψ(2S) production (left and right, respectively) as a function of p_{T} for different rapidity bins. The error bars on the data points include all the statistical and systematic contributions except luminosity and polarization. The measurements have been offset by the numerical values given in the legend for easier viewing. The coloured (dark) bands indicate the theoretical predictions from NRQCD calculations. The lines are added only for illustrative purposes.

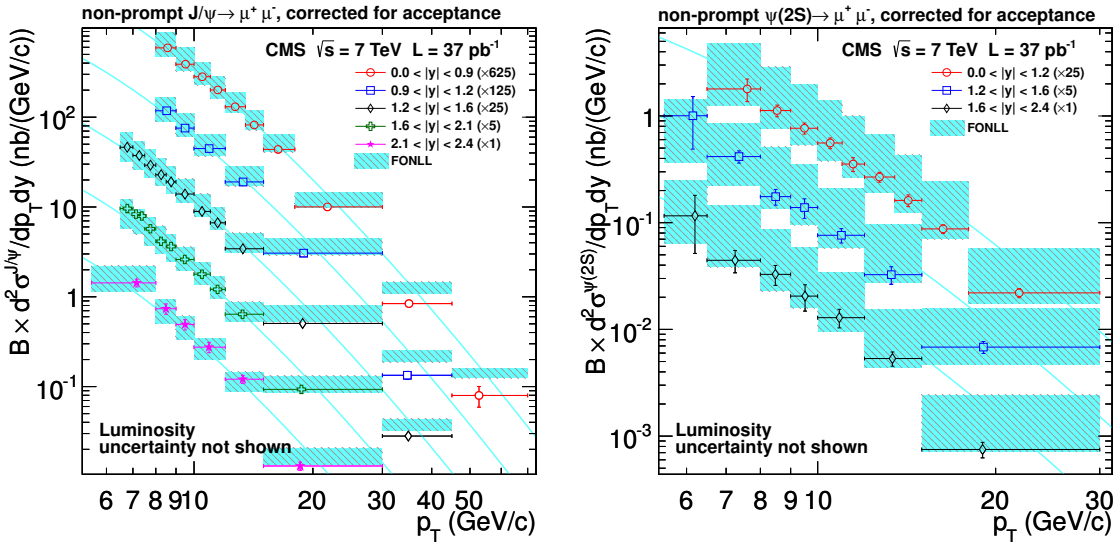

Figure 6. Measured differential cross section for non-prompt J/ψ and ψ(2S) production (left and right, respectively) as a function of p_{T} for different rapidity bins. The error bars on the data points include all the statistical and systematic contributions except luminosity. The measurements have been offset by the numerical values given in the legend for easier viewing. The coloured (dark) bands indicate the theoretical predictions from FONLL calculations. The lines are added only for illustrative purposes.

JHEP02(2012)011

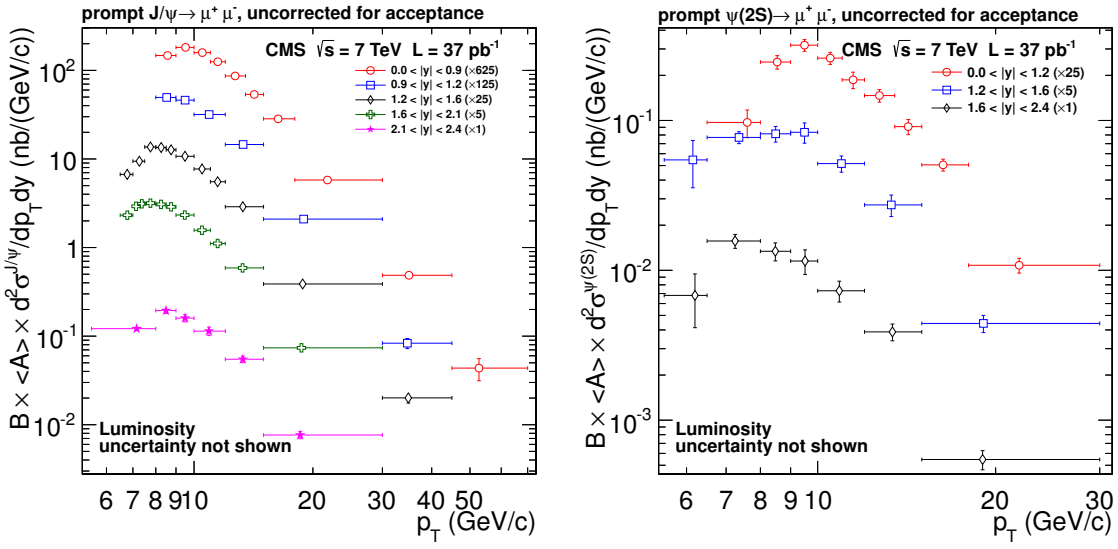

Figure 7. Measured differential cross section for prompt J/ψ (left) and $\psi(2S)$ (right) production as a function of p_T for the different rapidity bins. The error bars on data points include all the statistical and systematic contributions except luminosity. The measurements have been offset by the numerical values given in the legend for easier viewing. The results are not corrected for the muon acceptance.

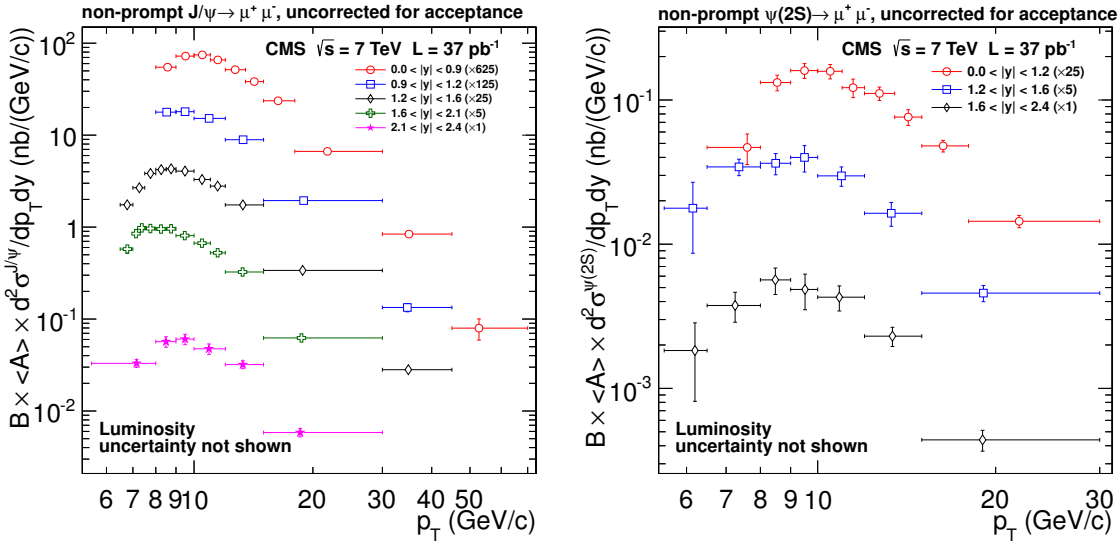

Figure 8. Measured differential cross section for non-prompt J/ψ (left) and $\psi(2S)$ (right) production as a function of p_T for the different rapidity bins. The error bars on data points include all the statistical and systematic contributions except luminosity. The measurements have been offset by the numerical values given in the legend for easier viewing. The result is not corrected for the muon acceptance.

cross sections:

$$R(p_T, |y|) = \frac{\frac{d^2\sigma}{dp_T dy}(\psi(2S)) \cdot \mathcal{B}(\psi(2S) \to \mu^+\mu^-)}{\frac{d^2\sigma}{dp_T dy}(J/\psi) \cdot \mathcal{B}(J/\psi \to \mu^+\mu^-)} = \frac{N^{corr}_{\psi(2S)}(p_T, |y|)}{N^{corr}_{J/\psi}(p_T, |y|)} \quad , \tag{9.1}$$

JHEP02(2012)011

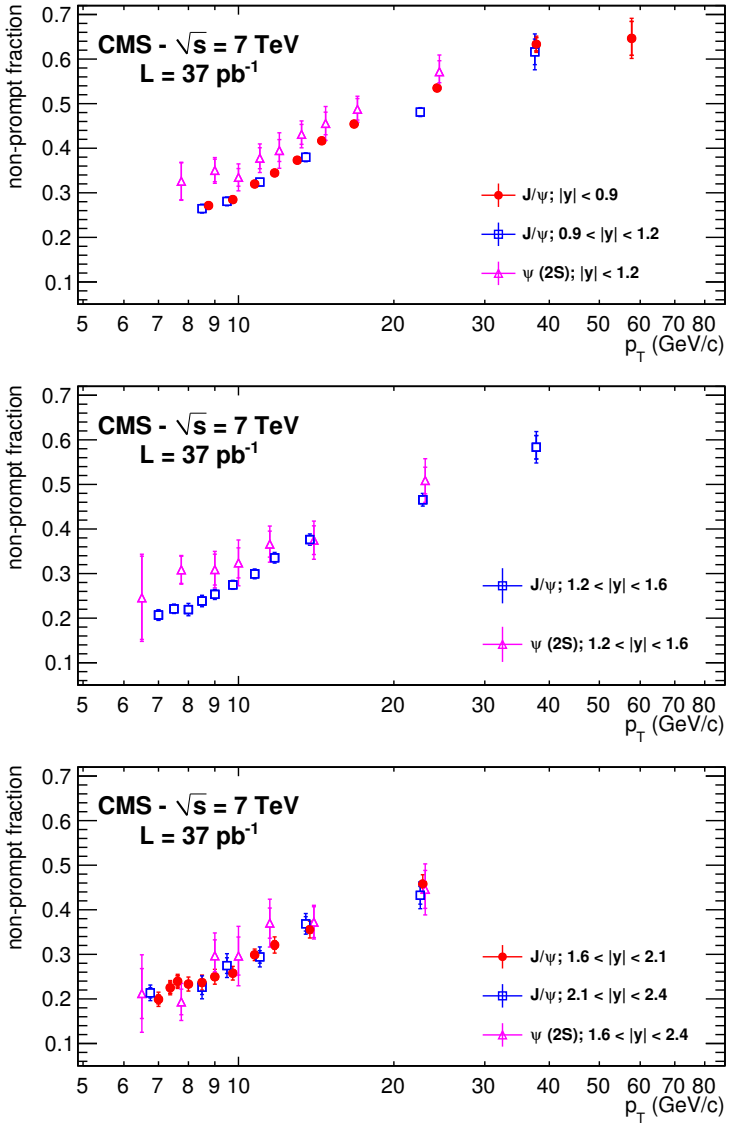

Figure 9. Fitted J/ψ and $\psi(2S)$ non-prompt fractions plotted as a function of p_T for three rapidity regions: $0 < |y| < 1.2$ (top); $1.2 < |y| < 1.6$ (middle); $1.6 < |y| < 2.4$ (bottom). The inner error bars represent the statistical uncertainties only, the outer ones are the quadratic sum of statistical and systematic uncertainties.

where the ratio R is computed in bins of p_T and rapidity, and the binning is the same as used for the $\psi(2S)$ cross section.

The statistical uncertainties affecting R are extracted directly from the simultaneous invariant mass fits. The systematic uncertainties are estimated by considering the same sources as for the cross sections (except the luminosity and single-muon efficiency, which cancel out in the ratio) and evaluating directly the variation of the ratio, in order to take correlations into account.

JHEP02(2012)011

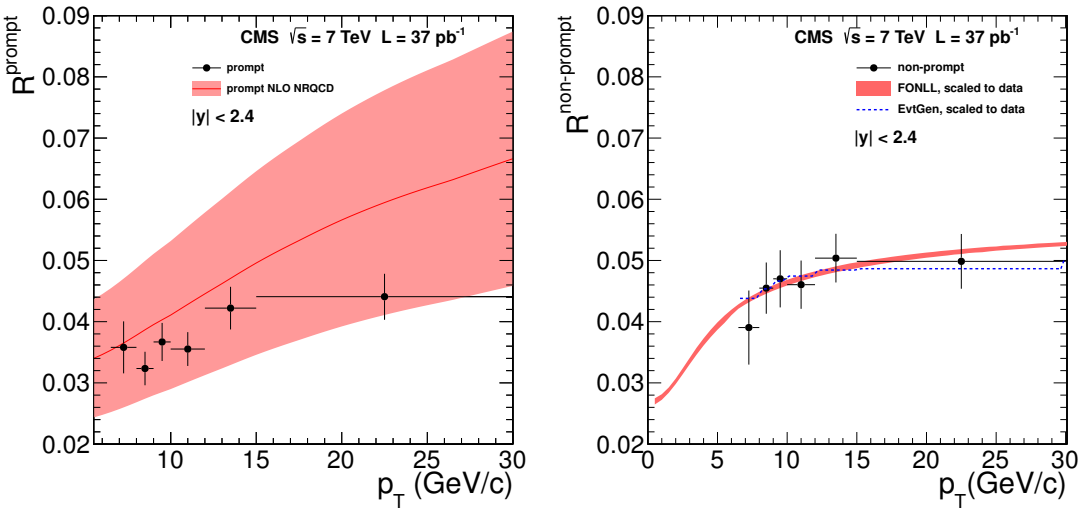

Figure 10. Measured value of R, the $\psi(2S)$ to J/ψ differential cross section ratio defined in eq. (9.1), for prompt (left) and non-prompt (right) production, averaged over rapidity and plotted as a function of p_T. The left plot also includes the comparison with the NRQCD prediction, while the right plot shows the predictions of the theoretical models used to determine $\mathcal{B}(B \to \psi(2S)X)$, after the latter have been rescaled to the fitted value given in eq. (9.2). The shaded bands show the uncertainties on the theoretical predictions. The error bars give the total uncertainties on the measurements; polarization uncertainties are not included.

No significant dependence of R on rapidity is observed; the ratios over the entire rapidity range are therefore computed. The resulting prompt and non-prompt cross section ratios are shown in figure 10 as a function of p_T. Numerical values of rapidity-dependent and integrated ratios are given in ref. [30].

The assumptions on polarization also affect the prompt cross section ratio measurement. In a plausible scenario [31], the polarizations of the directly produced J/ψ and $\psi(2S)$ states are assumed to be the same. Therefore the uncertainty on the ratio comes only from the difference between the polarization of the directly produced mesons and the polarization of the J/ψ coming from decays of P-wave states (χ_{c1} and χ_{c2}), for which the maximum possible variations are considered. Using the measured feed-down fractions measured at CDF [32, 33], this leads to the definition of the two extreme scenarios:

- $\lambda_\theta^{\psi(2S)} = 1$, $\lambda_\theta^{J/\psi} = 0.445$;
- $\lambda_\theta^{\psi(2S)} = -1$, $\lambda_\theta^{J/\psi} = -0.647$;

which result in changes to the measured prompt cross section ratio by $12 - 20\%$.

9.5 Inclusive $B \to \psi(2S)X$ branching fraction

The non-prompt $\psi(2S)$ cross section results can be used to determine $\mathcal{B}(B \to \psi(2S)X)$, the average inclusive branching fraction of all weakly decaying particles containing a b quark to $\psi(2S)$.

JHEP02(2012)011

Since the results are determined only for a limited range of phase space, a theoretical assumption is needed to extrapolate to the full phase space. The most precise result is obtained using the non-prompt cross section ratio, where most theoretical uncertainties cancel. The FONLL model is used for the result, taking as an alternative the EvtGen prediction to determine a systematic uncertainty.

For both models, the predicted ratio is computed for each p_{T} bin used in the measurement, assuming the world-average values, listed by the Particle Data Group (PDG) [24], of $\mathcal{B}_{\mathrm{PDG}}(\mathrm{B} \to J/\psi\, X)$, $\mathcal{B}_{\mathrm{PDG}}(\psi(2\mathrm{S}) \to \mu^+\mu^-)$, and $\mathcal{B}_{\mathrm{PDG}}(J/\psi \to \mu^+\mu^-)$ (the branching fractions taken from the PDG are indicated as $\mathcal{B}_{\mathrm{PDG}}$). In both models the production cross section for each type of B meson or baryon is weighted using the values of the fractions $f(\mathrm{b} \to \mathrm{B}^0)$, $f(\mathrm{b} \to \mathrm{B}^{\pm})$, $f(\mathrm{b} \to \mathrm{B}_s^0)$, and $f(\mathrm{b} \to \Lambda_{\mathrm{b}}^0)$, taken from LEP and Tevatron measurements. The predictions are then fitted to the data points, leaving only the normalization (N) as a free parameter. A good agreement in the shape of the p_{T} distribution is found for both models. The branching fraction $\mathcal{B}(\mathrm{B} \to \psi(2\mathrm{S})X)$ is then derived from the fitted normalization.

In addition to the fit uncertainty, including statistical and systematic uncertainties on the single measurements ($\pm 3.8\%$), the following sources of uncertainty are considered (with the corresponding relative $\Delta\mathcal{B}$ uncertainty given in parentheses):

- *PDG branching fractions.* The uncertainties quoted by the PDG for $\mathcal{B}(\mathrm{B} \to J/\psi\, X)$, $\mathcal{B}(\psi(2\mathrm{S}) \to \mu^+\mu^-)$, and $\mathcal{B}(J/\psi \to \mu^+\mu^-)$ are summed in quadrature (13.5%).

- *Model assumptions.* The EvtGen prediction is used for an alternative fit and the difference with respect to the nominal N value is taken as a systematic uncertainty (1.0%).

- *FONLL uncertainties.* All uncertainties on the underlying $b\bar{b}$ cross section, discussed in section 9.1, are assumed to be fully correlated between $\mathrm{B} \to J/\psi\, X$ and $\mathrm{B} \to \psi(2\mathrm{S})X$ transitions. Residual uncertainties affecting the cross section ratio prediction are used to perform alternative fits and the differences with respect to the nominal value of N are taken as systematic uncertainties (1.5%).

- $\mathrm{B} \to$ *charmonium spectrum theoretical uncertainties.* The only source of theoretical uncertainty which is not correlated is the one on the $\mathrm{B} \to$ charmonium spectrum. We use the high-Q and low-Q method to estimate this uncertainty as detailed in section 9.1. In order to obtain an upper limit on the uncertainty of this ratio, the high-Q sample of $\mathrm{B} \to J/\psi X$ is compared to the low-Q $\mathrm{B} \to \psi(2\mathrm{S})X$ sample and vice versa. The average difference in N with respect to the nominal EvtGen prediction is taken as a systematic uncertainty (3.8%).

The measured value is:

$$\mathcal{B}(\mathrm{B} \to \psi(2\mathrm{S})X) = (3.08 \pm 0.12(\mathrm{stat.+syst.}) \pm 0.13(\mathrm{theor.}) \pm 0.42(\mathcal{B}_{\mathrm{PDG}})) \times 10^{-3}, \quad (9.2)$$

where the last uncertainties are from the world-average branching fractions and the theoretical variations, respectively. The result is in agreement with the current world-average value from LEP and Tevatron measurements ($\mathcal{B}_{\mathrm{PDG}}(\mathrm{B} \to \psi(2\mathrm{S})X) = (4.8 \pm 2.4) \cdot 10^{-3}$ [24]), while improving the relative uncertainty by a factor of three.

JHEP02(2012)011

10 Summary

A measurement of the J/ψ and $\psi(2S)$ production cross sections in pp collisions at $\sqrt{s} = 7\,\text{TeV}$ with the CMS experiment at the LHC has been presented. The data sample corresponds to an integrated luminosity of $36.7 \pm 1.5\,\text{pb}^{-1}$. The two cross sections and their ratio have been measured as a function of the meson transverse momentum (up to $70\,\text{GeV}/c$ for the J/ψ and to $30\,\text{GeV}/c$ for the $\psi(2S)$) in several rapidity ranges. Cross sections for prompt and non-prompt production have been determined from the measured values of the J/ψ and $\psi(2S)$ non-prompt fractions.

The prompt cross section results are evaluated assuming isotropic decays in the production, as well as four other polarization scenarios. In addition, cross sections restricted to the acceptance of the CMS detector are given, which are not affected by the polarization of the charmonium states.

Cross sections for prompt and non-prompt production have been compared with NRQCD and FONLL predictions, respectively. Agreement is found in the prompt case: this is particularly remarkable in the $\psi(2S)$ case, where theoretical uncertainties are reduced because of the absence of feed-down from heavier charmonium states. In the non-prompt case, general agreement in shape is found for $\psi(2S)$ in the entire p_T range considered (up to $30\,\text{GeV}/c$), but an overall scale shift is observed, because of the assumption on the central value of the inclusive branching fraction $\mathcal{B}(B \to \psi(2S)X)$. For J/ψ there is similarly general agreement over the above range, while the predictions overestimate the measured differential cross sections for $30 < p_T < 70\,\text{GeV}/c$.

For plausible hypotheses on the polarizations of the two charmonium states the ratio of their differential cross sections is obtained. In this ratio systematic errors largely cancel. The inclusive branching fraction $\mathcal{B}(B \to \psi(2S)X)$ is extracted from the ratio of the non-prompt cross sections to be:

$$\mathcal{B}(B \to \psi(2S)X) = (3.08 \pm 0.12\,(\text{stat.+syst.}) \pm 0.13\,(\text{theor.}) \pm 0.42\,(\mathcal{B}_{\text{PDG}})) \times 10^{-3},$$

improving the relative uncertainty on the previous world average by a factor of three.

Acknowledgments

We would like to thank Yan-Qing Ma for providing theoretical predictions in NLO NRQCD and Matteo Cacciari for predictions in the FONLL scheme and useful discussions.

We wish to congratulate our colleagues in the CERN accelerator departments for the excellent performance of the LHC machine. We thank the technical and administrative staff at CERN and other CMS institutes. This work was supported by the Austrian Federal Ministry of Science and Research; the Belgium Fonds de la Recherche Scientifique, and Fonds voor Wetenschappelijk Onderzoek; the Brazilian Funding Agencies (CNPq, CAPES, FAPERJ, and FAPESP); the Bulgarian Ministry of Education and Science; CERN; the Chinese Academy of Sciences, Ministry of Science and Technology, and National Natural Science Foundation of China; the Colombian Funding Agency (COLCIENCIAS); the Croatian Ministry of Science, Education and Sport; the Research Promotion Foundation,

Cyprus; the Estonian Academy of Sciences and NICPB; the Academy of Finland, Finnish Ministry of Education and Culture, and Helsinki Institute of Physics; the Institut National de Physique Nucléaire et de Physique des Particules / CNRS, and Commissariat à l'Énergie Atomique et aux Énergies Alternatives / CEA, France; the Bundesministerium für Bildung und Forschung, Deutsche Forschungsgemeinschaft, and Helmholtz-Gemeinschaft Deutscher Forschungszentren, Germany; the General Secretariat for Research and Technology, Greece; the National Scientific Research Foundation, and National Office for Research and Technology, Hungary; the Department of Atomic Energy and the Department of Science and Technology, India; the Institute for Studies in Theoretical Physics and Mathematics, Iran; the Science Foundation, Ireland; the Istituto Nazionale di Fisica Nucleare, Italy; the Korean Ministry of Education, Science and Technology and the World Class University program of NRF, Korea; the Lithuanian Academy of Sciences; the Mexican Funding Agencies (CINVESTAV, CONACYT, SEP, and UASLP-FAI); the Ministry of Science and Innovation, New Zealand; the Pakistan Atomic Energy Commission; the State Commission for Scientific Research, Poland; the Fundação para a Ciência e a Tecnologia, Portugal; JINR (Armenia, Belarus, Georgia, Ukraine, Uzbekistan); the Ministry of Science and Technologies of the Russian Federation, the Russian Ministry of Atomic Energy and the Russian Foundation for Basic Research; the Ministry of Science and Technological Development of Serbia; the Ministerio de Ciencia e Innovación, and Programa Consolider-Ingenio 2010, Spain; the Swiss Funding Agencies (ETH Board, ETH Zurich, PSI, SNF, UniZH, Canton Zurich, and SER); the National Science Council, Taipei; the Scientific and Technical Research Council of Turkey, and Turkish Atomic Energy Authority; the Science and Technology Facilities Council, U.K.; the US Department of Energy, and the US National Science Foundation.

Individuals have received support from the Marie-Curie programme and the European Research Council (European Union); the Leventis Foundation; the A. P. Sloan Foundation; the Alexander von Humboldt Foundation; the Belgian Federal Science Policy Office; the Fonds pour la Formation à la Recherche dans l'Industrie et dans l'Agriculture (FRIA-Belgium); the Agentschap voor Innovatie door Wetenschap en Technologie (IWT-Belgium); and the Council of Science and Industrial Research, India.

References

[1] P. Artoisenet, J. Lansberg and F. Maltoni, *Hadroproduction of J/ψ and υ in association with a heavy-quark pair*, *Phys. Lett.* **B 653** (2007) 60 [hep-ph/0703129] [INSPIRE].

[2] P. Artoisenet, F. Maltoni and T. Stelzer, *Automatic generation of quarkonium amplitudes in NRQCD*, *JHEP* **02** (2008) 102 [arXiv:0712.2770] [INSPIRE].

[3] Y.-Q. Ma, K. Wang and K.-T. Chao, *J/ψ (ψ) production at the Tevatron and LHC at $O(\alpha_s^4 v^4)$ in nonrelativistic QCD*, *Phys. Rev. Lett.* **106** (2011) 042002 [arXiv:1009.3655] [INSPIRE].

JHEP02(2012)011

[4] CDF collaboration, T. Aaltonen et al., *Production of $\Psi(2S)$ mesons in $p\bar{p}$ collisions at 1.96 TeV*, *Phys. Rev.* **D 80** (2009) 031103 [arXiv:0905.1982] [INSPIRE].

[5] M. Cacciari, M. Greco and P. Nason, *The p_T spectrum in heavy flavor hadroproduction*, *JHEP* **05** (1998) 007 [hep-ph/9803400] [INSPIRE].

[6] M. Cacciari, S. Frixione and P. Nason, *The p_T spectrum in heavy flavor photoproduction*, *JHEP* **03** (2001) 006 [hep-ph/0102134] [INSPIRE].

[7] CMS collaboration, V. Khachatryan et al., *Prompt and non-prompt J/ψ production in pp collisions at $\sqrt{s} = 7$ TeV*, *Eur. Phys. J.* **C 71** (2011) 1575 [arXiv:1011.4193] [INSPIRE].

[8] ATLAS collaboration, G. Aad et al., *Measurement of the differential cross-sections of inclusive, prompt and non-prompt J/psi production in proton-proton collisions at sqrt(s) = 7 TeV*, *Nucl. Phys.* **B 850** (2011) 387 [arXiv:1104.3038] [INSPIRE].

[9] LHCb collaboration, R. Aaij et al., *Measurement of J/ψ production in pp collisions at $\sqrt{s} = 7$ TeV*, *Eur. Phys. J.* **C 71** (2011) 1645 [arXiv:1103.0423] [INSPIRE].

[10] ALICE collaboration, K. Aamodt et al., *Rapidity and transverse momentum dependence of inclusive J/ψ production in pp collisions at $\sqrt{s} = 7$ TeV*, *Phys. Lett.* **B 704** (2011) 442 [arXiv:1105.0380] [INSPIRE].

[11] D. Lange, *The* EvtGen *particle decay simulation package*, *Nucl. Instrum. Meth.* **A 462** (2001) 152 [INSPIRE].

[12] BABAR collaboration, B. Aubert et al., *Study of inclusive production of charmonium mesons in B decay*, *Phys. Rev.* **D 67** (2003) 032002 [hep-ex/0207097] [INSPIRE].

[13] CMS collaboration, R. Adolphi et al., *The CMS experiment at the CERN LHC*, 2008 *JINST* **3** S08004 [INSPIRE].

[14] CMS collaboration, *Absolute luminosity normalization*, CMS-DP-2011-002 (2011).

[15] T. Sjöstrand, S. Mrenna and P.Z. Skands, PYTHIA *6.4 physics and manual*, *JHEP* **05** (2006) 026 [hep-ph/0603175] [INSPIRE].

[16] M. Krämer, *Quarkonium production at high-energy colliders*, *Prog. Part. Nucl. Phys.* **47** (2001) 141 [hep-ph/0106120] [INSPIRE].

[17] M. Bargiotti and V. Vagnoni, *Heavy quarkonia sector in* PYTHIA *6.324: tuning, validation and perspectives at LHC(b)*, *CERN report* **LHCb-2007-042** (2007).

[18] E. Barberio, B. van Eijk and Z. Was, PHOTOS*: a universal Monte Carlo for QED radiative corrections in decays*, *Comput. Phys. Commun.* **66** (1991) 115 [INSPIRE].

[19] E. Barberio and Z. Was, PHOTOS*: a universal Monte Carlo for QED radiative corrections. Version 2.0*, *Comput. Phys. Commun.* **79** (1994) 291 [INSPIRE].

[20] CMS collaboration, S. Chatrchyan et al., *Precise mapping of the magnetic field in the CMS barrel yoke using cosmic rays*, 2010 *JINST* **5** T03021 [arXiv:0910.5530] [INSPIRE].

[21] CMS collaboration, *Studies of tracker material*, PAS-TRK-10-003.

[22] CMS collaboration, S. Chatrchyan et al., *Alignment of the CMS silicon tracker during commissioning with cosmic rays*, 2010 *JINST* **5** T03009 [arXiv:0910.2505] [INSPIRE].

[23] J.E. Gaiser, *Charmonium spectroscopy from radiative decays of the J/ψ and ψ'*, Ph.D. Thesis, SLAC, Stanford U.S.A. (1982) [SLAC-R-255, appendix F].

JHEP02(2012)011

[24] Particle Data Group collaboration, K. Nakamura et al., *Review of particle physics*, *J. Phys.* **G 37** (2010) 075021 [INSPIRE].

[25] P. Faccioli, C. Lourenco, J. Seixas and H.K. Wohri, *Towards the experimental clarification of quarkonium polarization*, *Eur. Phys. J.* **C 69** (2010) 657 [arXiv:1006.2738] [INSPIRE].

[26] CMS collaboration, *Measurement of momentum scale and resolution of the CMS detector using low-mass resonances and cosmic ray muons*, PAS-TRK-10-004.

[27] CMS collaboration, *Performance of muon identification in pp collisions at* $\sqrt{s} = 7$ *TeV*, PAS-MUO-10-002.

[28] CMS collaboration, *Measurement of tracking efficiency*, PAS-TRK-10-002.

[29] G. Punzi, *Comments on likelihood fits with variable resolution*, *eConf* **C 030908** (2003) WELT002 [physics/0401045] [INSPIRE].

[30] CMS collaboration, *Numerical result of the data presented in this paper*, available at *JHEP* **02** (2012) 011 as supplement material.

[31] P. Faccioli, C. Lourenço, J. Seixas and H.K. Wöhri, *Determination of* χ_c *and* χ_b *polarizations from dilepton angular distributions in radiative decays*, *Phys. Rev.* **D 83** (2011) 096001 [arXiv:1103.4882] [INSPIRE].

[32] CDF collaboration, F. Abe et al., *Production of* J/ψ *mesons from* χ_c *meson decays in* $p\bar{p}$ *collisions at* $\sqrt{s} = 1.8$ *TeV*, *Phys. Rev. Lett.* **79** (1997) 578 [INSPIRE].

[33] CDF collaboration, A. Abulencia et al., *Measurement of* $\sigma_{\chi_{c2}}\mathcal{B}(\chi_{c2} \to J/\psi\gamma)/\sigma_{\chi_{c1}}\mathcal{B}(\chi_{c1} \to J/\psi\gamma)$ *in* $p\bar{p}$ *collisions at* $\sqrt{s} = 1.96$ *TeV*, *Phys. Rev. Lett.* **98** (2007) 232001 [hep-ex/0703028] [INSPIRE].

JHEP02(2012)011

The CMS collaboration

Yerevan Physics Institute, Yerevan, Armenia

S. Chatrchyan, V. Khachatryan, A.M. Sirunyan, A. Tumasyan

Institut für Hochenergiephysik der OeAW, Wien, Austria

W. Adam, T. Bergauer, M. Dragicevic, J. Erö, C. Fabjan, M. Friedl, R. Frühwirth, V.M. Ghete, J. Hammer[1], M. Hoch, N. Hörmann, J. Hrubec, M. Jeitler, W. Kiesenhofer, M. Krammer, D. Liko, I. Mikulec, M. Pernicka, B. Rahbaran, H. Rohringer, R. Schöfbeck, J. Strauss, A. Taurok, F. Teischinger, C. Trauner, P. Wagner, W. Waltenberger, G. Walzel, E. Widl, C.-E. Wulz

National Centre for Particle and High Energy Physics, Minsk, Belarus

V. Mossolov, N. Shumeiko, J. Suarez Gonzalez

Universiteit Antwerpen, Antwerpen, Belgium

S. Bansal, L. Benucci, E.A. De Wolf, X. Janssen, S. Luyckx, T. Maes, L. Mucibello, S. Ochesanu, B. Roland, R. Rougny, M. Selvaggi, H. Van Haevermaet, P. Van Mechelen, N. Van Remortel

Vrije Universiteit Brussel, Brussel, Belgium

F. Blekman, S. Blyweert, J. D'Hondt, R. Gonzalez Suarez, A. Kalogeropoulos, M. Maes, A. Olbrechts, W. Van Doninck, P. Van Mulders, G.P. Van Onsem, I. Villella

Université Libre de Bruxelles, Bruxelles, Belgium

O. Charaf, B. Clerbaux, G. De Lentdecker, V. Dero, A.P.R. Gay, G.H. Hammad, T. Hreus, A. Léonard, P.E. Marage, L. Thomas, C. Vander Velde, P. Vanlaer, J. Wickens

Ghent University, Ghent, Belgium

V. Adler, K. Beernaert, A. Cimmino, S. Costantini, M. Grunewald, B. Klein, J. Lellouch, A. Marinov, J. Mccartin, D. Ryckbosch, N. Strobbe, F. Thyssen, M. Tytgat, L. Vanelderen, P. Verwilligen, S. Walsh, N. Zaganidis

Université Catholique de Louvain, Louvain-la-Neuve, Belgium

S. Basegmez, G. Bruno, J. Caudron, L. Ceard, E. Cortina Gil, J. De Favereau De Jeneret, C. Delaere, D. Favart, L. Forthomme, A. Giammanco[2], G. Grégoire, J. Hollar, V. Lemaitre, J. Liao, O. Militaru, C. Nuttens, S. Ovyn, D. Pagano, A. Pin, K. Piotrzkowski, N. Schul

Université de Mons, Mons, Belgium

N. Beliy, T. Caebergs, E. Daubie

Centro Brasileiro de Pesquisas Fisicas, Rio de Janeiro, Brazil

G.A. Alves, D. De Jesus Damiao, M.E. Pol, M.H.G. Souza

JHEP02(2012)011

Universidade do Estado do Rio de Janeiro, Rio de Janeiro, Brazil

W.L. Aldá Júnior, W. Carvalho, A. Custódio, E.M. Da Costa, C. De Oliveira Martins, S. Fonseca De Souza, D. Matos Figueiredo, L. Mundim, H. Nogima, V. Oguri, W.L. Prado Da Silva, A. Santoro, S.M. Silva Do Amaral, A. Sznajder

Instituto de Fisica Teorica, Universidade Estadual Paulista, Sao Paulo, Brazil

T.S. Anjos[3], C.A. Bernardes[3], F.A. Dias[4], T.R. Fernandez Perez Tomei, E. M. Gregores[3], C. Lagana, F. Marinho, P.G. Mercadante[3], S.F. Novaes, Sandra S. Padula

Institute for Nuclear Research and Nuclear Energy, Sofia, Bulgaria

N. Darmenov[1], V. Genchev[1], P. Iaydjiev[1], S. Piperov, M. Rodozov, S. Stoykova, G. Sultanov, V. Tcholakov, R. Trayanov, M. Vutova

University of Sofia, Sofia, Bulgaria

A. Dimitrov, R. Hadjiiska, A. Karadzhinova, V. Kozhuharov, L. Litov, M. Mateev, B. Pavlov, P. Petkov

Institute of High Energy Physics, Beijing, China

J.G. Bian, G.M. Chen, H.S. Chen, C.H. Jiang, D. Liang, S. Liang, X. Meng, J. Tao, J. Wang, J. Wang, X. Wang, Z. Wang, H. Xiao, M. Xu, J. Zang, Z. Zhang

State Key Lab. of Nucl. Phys. and Tech., Peking University, Beijing, China

Y. Ban, S. Guo, Y. Guo, W. Li, Y. Mao, S.J. Qian, H. Teng, B. Zhu, W. Zou

Universidad de Los Andes, Bogota, Colombia

A. Cabrera, B. Gomez Moreno, A.A. Ocampo Rios, A.F. Osorio Oliveros, J.C. Sanabria

Technical University of Split, Split, Croatia

N. Godinovic, D. Lelas, R. Plestina[5], D. Polic, I. Puljak

University of Split, Split, Croatia

Z. Antunovic, M. Dzelalija, M. Kovac

Institute Rudjer Boskovic, Zagreb, Croatia

V. Brigljevic, S. Duric, K. Kadija, J. Luetic, S. Morovic

University of Cyprus, Nicosia, Cyprus

A. Attikis, M. Galanti, J. Mousa, C. Nicolaou, F. Ptochos, P.A. Razis

Charles University, Prague, Czech Republic

M. Finger, M. Finger Jr.

JHEP02(2012)011

Academy of Scientific Research and Technology of the Arab Republic of Egypt, Egyptian Network of High Energy Physics, Cairo, Egypt

Y. Assran[6], A. Ellithi Kamel[7], S. Khalil[8], M.A. Mahmoud[9], A. Radi[10]

National Institute of Chemical Physics and Biophysics, Tallinn, Estonia

A. Hektor, M. Kadastik, M. Müntel, M. Raidal, L. Rebane, A. Tiko

Department of Physics, University of Helsinki, Helsinki, Finland

V. Azzolini, P. Eerola, G. Fedi, M. Voutilainen

Helsinki Institute of Physics, Helsinki, Finland

S. Czellar, J. Härkönen, A. Heikkinen, V. Karimäki, R. Kinnunen, M.J. Kortelainen, T. Lampén, K. Lassila-Perini, S. Lehti, T. Lindén, P. Luukka, T. Mäenpää, E. Tuominen, J. Tuominiemi, E. Tuovinen, D. Ungaro, L. Wendland

Lappeenranta University of Technology, Lappeenranta, Finland

K. Banzuzi, A. Karjalainen, A. Korpela, T. Tuuva

Laboratoire d'Annecy-le-Vieux de Physique des Particules, IN2P3-CNRS, Annecy-le-Vieux, France

D. Sillou

DSM/IRFU, CEA/Saclay, Gif-sur-Yvette, France

M. Besancon, S. Choudhury, M. Dejardin, D. Denegri, B. Fabbro, J.L. Faure, F. Ferri, S. Ganjour, A. Givernaud, P. Gras, G. Hamel de Monchenault, P. Jarry, E. Locci, J. Malcles, M. Marionneau, L. Millischer, J. Rander, A. Rosowsky, I. Shreyber, M. Titov

Laboratoire Leprince-Ringuet, Ecole Polytechnique, IN2P3-CNRS, Palaiseau, France

S. Baffioni, F. Beaudette, L. Benhabib, L. Bianchini, M. Bluj[11], C. Broutin, P. Busson, C. Charlot, T. Dahms, L. Dobrzynski, S. Elgammal, R. Granier de Cassagnac, M. Haguenauer, P. Miné, C. Mironov, C. Ochando, P. Paganini, D. Sabes, R. Salerno, Y. Sirois, C. Thiebaux, C. Veelken, A. Zabi

Institut Pluridisciplinaire Hubert Curien, Université de Strasbourg, Université de Haute Alsace Mulhouse, CNRS/IN2P3, Strasbourg, France

J.-L. Agram[12], J. Andrea, D. Bloch, D. Bodin, J.-M. Brom, M. Cardaci, E.C. Chabert, C. Collard, E. Conte[12], F. Drouhin[12], C. Ferro, J.-C. Fontaine[12], D. Gelé, U. Goerlach, S. Greder, P. Juillot, M. Karim[12], A.-C. Le Bihan, P. Van Hove

Centre de Calcul de l'Institut National de Physique Nucleaire et de Physique des Particules (IN2P3), Villeurbanne, France

F. Fassi, D. Mercier

JHEP02(2012)011

Université de Lyon, Université Claude Bernard Lyon 1, CNRS-IN2P3, Institut de Physique Nucléaire de Lyon, Villeurbanne, France

C. Baty, S. Beauceron, N. Beaupere, M. Bedjidian, O. Bondu, G. Boudoul, D. Boumediene, H. Brun, J. Chasserat, R. Chierici, D. Contardo, P. Depasse, H. El Mamouni, A. Falkiewicz, J. Fay, S. Gascon, B. Ille, T. Kurca, T. Le Grand, M. Lethuillier, L. Mirabito, S. Perries, V. Sordini, S. Tosi, Y. Tschudi, P. Verdier, S. Viret

Institute of High Energy Physics and Informatization, Tbilisi State University, Tbilisi, Georgia

D. Lomidze

RWTH Aachen University, I. Physikalisches Institut, Aachen, Germany

G. Anagnostou, S. Beranek, M. Edelhoff, L. Feld, N. Heracleous, O. Hindrichs, R. Jussen, K. Klein, J. Merz, A. Ostapchuk, A. Perieanu, F. Raupach, J. Sammet, S. Schael, D. Sprenger, H. Weber, M. Weber, B. Wittmer, V. Zhukov[13]

RWTH Aachen University, III. Physikalisches Institut A, Aachen, Germany

M. Ata, E. Dietz-Laursonn, M. Erdmann, T. Hebbeker, C. Heidemann, A. Hinzmann, K. Hoepfner, T. Klimkovich, D. Klingebiel, P. Kreuzer, D. Lanske†, J. Lingemann, C. Magass, M. Merschmeyer, A. Meyer, P. Papacz, H. Pieta, H. Reithler, S.A. Schmitz, L. Sonnenschein, J. Steggemann, D. Teyssier

RWTH Aachen University, III. Physikalisches Institut B, Aachen, Germany

M. Bontenackels, V. Cherepanov, M. Davids, G. Flügge, H. Geenen, M. Giffels, W. Haj Ahmad, F. Hoehle, B. Kargoll, T. Kress, Y. Kuessel, A. Linn, A. Nowack, L. Perchalla, O. Pooth, J. Rennefeld, P. Sauerland, A. Stahl, D. Tornier, M.H. Zoeller

Deutsches Elektronen-Synchrotron, Hamburg, Germany

M. Aldaya Martin, W. Behrenhoff, U. Behrens, M. Bergholz[14], A. Bethani, K. Borras, A. Cakir, A. Campbell, E. Castro, D. Dammann, G. Eckerlin, D. Eckstein, A. Flossdorf, G. Flucke, A. Geiser, J. Hauk, H. Jung[1], M. Kasemann, P. Katsas, C. Kleinwort, H. Kluge, A. Knutsson, M. Krämer, D. Krücker, E. Kuznetsova, W. Lange, W. Lohmann[14], B. Lutz, R. Mankel, I. Marfin, M. Marienfeld, I.-A. Melzer-Pellmann, A.B. Meyer, J. Mnich, A. Mussgiller, S. Naumann-Emme, J. Olzem, A. Petrukhin, D. Pitzl, A. Raspereza, M. Rosin, R. Schmidt[14], T. Schoerner-Sadenius, N. Sen, A. Spiridonov, M. Stein, J. Tomaszewska, R. Walsh, C. Wissing

University of Hamburg, Hamburg, Germany

C. Autermann, V. Blobel, S. Bobrovskyi, J. Draeger, H. Enderle, U. Gebbert, M. Görner, T. Hermanns, K. Kaschube, G. Kaussen, H. Kirschenmann, R. Klanner, J. Lange, B. Mura, F. Nowak, N. Pietsch, C. Sander, H. Schettler, P. Schleper, E. Schlieckau, M. Schröder, T. Schum, H. Stadie, G. Steinbrück, J. Thomsen

JHEP02(2012)011

Institut für Experimentelle Kernphysik, Karlsruhe, Germany

C. Barth, J. Bauer, J. Berger, V. Buege, T. Chwalek, W. De Boer, A. Dierlamm, G. Dirkes, M. Feindt, J. Gruschke, M. Guthoff[1], C. Hackstein, F. Hartmann, M. Heinrich, H. Held, K.H. Hoffmann, S. Honc, I. Katkov[13], J.R. Komaragiri, T. Kuhr, D. Martschei, S. Mueller, Th. Müller, M. Niegel, O. Oberst, A. Oehler, J. Ott, T. Peiffer, G. Quast, K. Rabbertz, F. Ratnikov, N. Ratnikova, M. Renz, S. Röcker, C. Saout, A. Scheurer, P. Schieferdecker, F.-P. Schilling, M. Schmanau, G. Schott, H.J. Simonis, F.M. Stober, D. Troendle, J. Wagner-Kuhr, T. Weiler, M. Zeise, E.B. Ziebarth

Institute of Nuclear Physics "Demokritos", Aghia Paraskevi, Greece

G. Daskalakis, T. Geralis, S. Kesisoglou, A. Kyriakis, D. Loukas, I. Manolakos, A. Markou, C. Markou, C. Mavrommatis, E. Ntomari, E. Petrakou

University of Athens, Athens, Greece

L. Gouskos, T.J. Mertzimekis, A. Panagiotou, N. Saoulidou, E. Stiliaris

University of Ioánnina, Ioánnina, Greece

I. Evangelou, C. Foudas[1], P. Kokkas, N. Manthos, I. Papadopoulos, V. Patras, F.A. Triantis

KFKI Research Institute for Particle and Nuclear Physics, Budapest, Hungary

A. Aranyi, G. Bencze, L. Boldizsar, C. Hajdu[1], P. Hidas, D. Horvath[15], A. Kapusi, K. Krajczar[16], F. Sikler[1], G.I. Veres[16], G. Vesztergombi[16]

Institute of Nuclear Research ATOMKI, Debrecen, Hungary

N. Beni, J. Molnar, J. Palinkas, Z. Szillasi, V. Veszpremi

University of Debrecen, Debrecen, Hungary

J. Karancsi, P. Raics, Z.L. Trocsanyi, B. Ujvari

Panjab University, Chandigarh, India

S.B. Beri, V. Bhatnagar, N. Dhingra, R. Gupta, M. Jindal, M. Kaur, J.M. Kohli, M.Z. Mehta, N. Nishu, L.K. Saini, A. Sharma, A.P. Singh, J. Singh, S.P. Singh

University of Delhi, Delhi, India

S. Ahuja, B.C. Choudhary, P. Gupta, A. Kumar, A. Kumar, S. Malhotra, M. Naimuddin, K. Ranjan, R.K. Shivpuri

Saha Institute of Nuclear Physics, Kolkata, India

S. Banerjee, S. Bhattacharya, S. Dutta, B. Gomber, S. Jain, S. Jain, R. Khurana, S. Sarkar

Bhabha Atomic Research Centre, Mumbai, India

R.K. Choudhury, D. Dutta, S. Kailas, V. Kumar, A.K. Mohanty[1], L.M. Pant, P. Shukla

JHEP02(2012)011

Tata Institute of Fundamental Research - EHEP, Mumbai, India

T. Aziz, M. Guchait[17], A. Gurtu, M. Maity[18], D. Majumder, G. Majumder, K. Mazumdar, G.B. Mohanty, B. Parida, A. Saha, K. Sudhakar, N. Wickramage

Tata Institute of Fundamental Research - HECR, Mumbai, India

S. Banerjee, S. Dugad, N.K. Mondal

Institute for Research and Fundamental Sciences (IPM), Tehran, Iran

H. Arfaei, H. Bakhshiansohi[19], S.M. Etesami[20], A. Fahim[19], M. Hashemi, H. Hesari, A. Jafari[19], M. Khakzad, A. Mohammadi[21], M. Mohammadi Najafabadi, S. Paktinat Mehdiabadi, B. Safarzadeh[22], M. Zeinali[20]

INFN Sezione di Bari[a], Università di Bari[b], Politecnico di Bari[c], Bari, Italy

M. Abbrescia[a,b], L. Barbone[a,b], C. Calabria[a,b], A. Colaleo[a], D. Creanza[a,c], N. De Filippis[a,c,1], M. De Palma[a,b], L. Fiore[a], G. Iaselli[a,c], L. Lusito[a,b], G. Maggi[a,c], M. Maggi[a], N. Manna[a,b], B. Marangelli[a,b], S. My[a,c], S. Nuzzo[a,b], N. Pacifico[a,b], A. Pompili[a,b], G. Pugliese[a,c], F. Romano[a,c], G. Selvaggi[a,b], L. Silvestris[a], S. Tupputi[a,b], G. Zito[a]

INFN Sezione di Bologna[a], Università di Bologna[b], Bologna, Italy

G. Abbiendi[a], A.C. Benvenuti[a], D. Bonacorsi[a], S. Braibant-Giacomelli[a,b], L. Brigliadori[a], P. Capiluppi[a,b], A. Castro[a,b], F.R. Cavallo[a], M. Cuffiani[a,b], G.M. Dallavalle[a], F. Fabbri[a], A. Fanfani[a,b], D. Fasanella[a,1], P. Giacomelli[a], M. Giunta[a], C. Grandi[a], S. Marcellini[a], G. Masetti[a], M. Meneghelli[a,b], A. Montanari[a], F.L. Navarria[a,b], F. Odorici[a], A. Perrotta[a], F. Primavera[a], A.M. Rossi[a,b], T. Rovelli[a,b], G. Siroli[a,b], R. Travaglini[a,b]

INFN Sezione di Catania[a], Università di Catania[b], Catania, Italy

S. Albergo[a,b], G. Cappello[a,b], M. Chiorboli[a,b], S. Costa[a,b], R. Potenza[a,b], A. Tricomi[a,b], C. Tuve[a,b]

INFN Sezione di Firenze[a], Università di Firenze[b], Firenze, Italy

G. Barbagli[a], V. Ciulli[a,b], C. Civinini[a], R. D'Alessandro[a,b], E. Focardi[a,b], S. Frosali[a,b], E. Gallo[a], S. Gonzi[a,b], M. Meschini[a], S. Paoletti[a], G. Sguazzoni[a], A. Tropiano[a,1]

INFN Laboratori Nazionali di Frascati, Frascati, Italy

L. Benussi, S. Bianco, S. Colafranceschi[23], F. Fabbri, D. Piccolo

INFN Sezione di Genova, Genova, Italy

P. Fabbricatore, R. Musenich

JHEP02(2012)011

INFN Sezione di Milano-Bicocca[a], Università di Milano-Bicocca[b], Milano, Italy

A. Benaglia[a,b,1], F. De Guio[a,b], L. Di Matteo[a,b], S. Gennai[a,1], A. Ghezzi[a,b], S. Malvezzi[a], A. Martelli[a,b], A. Massironi[a,b,1], D. Menasce[a], L. Moroni[a], M. Paganoni[a,b], D. Pedrini[a], S. Ragazzi[a,b], N. Redaelli[a], S. Sala[a], T. Tabarelli de Fatis[a,b]

INFN Sezione di Napoli[a], Università di Napoli "Federico II"[b], Napoli, Italy

S. Buontempo[a], C.A. Carrillo Montoya[a,1], N. Cavallo[a,24], A. De Cosa[a,b], O. Dogangun[a,b], F. Fabozzi[a,24], A.O.M. Iorio[a,1], L. Lista[a], M. Merola[a,b], P. Paolucci[a]

INFN Sezione di Padova[a], Università di Padova[b], Università di Trento (Trento)[c], Padova, Italy

P. Azzi[a], N. Bacchetta[a,1], P. Bellan[a,b], D. Bisello[a,b], A. Branca[a], R. Carlin[a,b], P. Checchia[a], T. Dorigo[a], U. Dosselli[a], F. Fanzago[a], F. Gasparini[a,b], U. Gasparini[a,b], A. Gozzelino[a], S. Lacaprara[a,25], I. Lazzizzera[a,c], M. Margoni[a,b], M. Mazzucato[a], A.T. Meneguzzo[a,b], M. Nespolo[a,1], L. Perrozzi[a], N. Pozzobon[a,b], P. Ronchese[a,b], F. Simonetto[a,b], E. Torassa[a], M. Tosi[a,b,1], S. Vanini[a,b], P. Zotto[a,b], G. Zumerle[a,b]

INFN Sezione di Pavia[a], Università di Pavia[b], Pavia, Italy

P. Baesso[a,b], U. Berzano[a], S.P. Ratti[a,b], C. Riccardi[a,b], P. Torre[a,b], P. Vitulo[a,b], C. Viviani[a,b]

INFN Sezione di Perugia[a], Università di Perugia[b], Perugia, Italy

M. Biasini[a,b], G.M. Bilei[a], B. Caponeri[a,b], L. Fanò[a,b], P. Lariccia[a,b], A. Lucaroni[a,b,1], G. Mantovani[a,b], M. Menichelli[a], A. Nappi[a,b], F. Romeo[a,b], A. Santocchia[a,b], S. Taroni[a,b,1], M. Valdata[a,b]

INFN Sezione di Pisa[a], Università di Pisa[b], Scuola Normale Superiore di Pisa[c], Pisa, Italy

P. Azzurri[a,c], G. Bagliesi[a], J. Bernardini[a,b], T. Boccali[a], G. Broccolo[a,c], R. Castaldi[a], R.T. D'Agnolo[a,c], R. Dell'Orso[a], F. Fiori[a,b], L. Foà[a,c], A. Giassi[a], A. Kraan[a], F. Ligabue[a,c], T. Lomtadze[a], L. Martini[a,26], A. Messineo[a,b], F. Palla[a], F. Palmonari[a], A. Rizzi, G. Segneri[a], A.T. Serban[a], P. Spagnolo[a], R. Tenchini[a], G. Tonelli[a,b,1], A. Venturi[a,1], P.G. Verdini[a]

INFN Sezione di Roma[a], Università di Roma "La Sapienza"[b], Roma, Italy

L. Barone[a,b], F. Cavallari[a], D. Del Re[a,b,1], M. Diemoz[a], D. Franci[a,b], M. Grassi[a,1], E. Longo[a,b], P. Meridiani[a], S. Nourbakhsh[a], G. Organtini[a,b], F. Pandolfi[a,b], R. Paramatti[a], S. Rahatlou[a,b], M. Sigamani[a]

JHEP02(2012)011

INFN Sezione di Torino[a], Università di Torino[b], Università del Piemonte Orientale (Novara)[c], Torino, Italy

N. Amapane[a,b], R. Arcidiacono[a,c], S. Argiro[a,b], M. Arneodo[a,c], C. Biino[a], C. Botta[a,b], N. Cartiglia[a], R. Castello[a,b], M. Costa[a,b], N. Demaria[a], A. Graziano[a,b], C. Mariotti[a], S. Maselli[a], E. Migliore[a,b], V. Monaco[a,b], M. Musich[a], M.M. Obertino[a,c], N. Pastrone[a], M. Pelliccioni[a], A. Potenza[a,b], A. Romero[a,b], M. Ruspa[a,c], R. Sacchi[a,b], V. Sola[a,b], A. Solano[a,b], A. Staiano[a], A. Vilela Pereira[a]

INFN Sezione di Trieste[a], Università di Trieste[b], Trieste, Italy

S. Belforte[a], F. Cossutti[a], G. Della Ricca[a,b], B. Gobbo[a], M. Marone[a,b], D. Montanino[a,b,1], A. Penzo[a]

Kangwon National University, Chunchon, Korea

S.G. Heo, S.K. Nam

Kyungpook National University, Daegu, Korea

S. Chang, J. Chung, D.H. Kim, G.N. Kim, J.E. Kim, D.J. Kong, H. Park, S.R. Ro, D.C. Son, T. Son

Chonnam National University, Institute for Universe and Elementary Particles, Kwangju, Korea

J.Y. Kim, Zero J. Kim, S. Song

Konkuk University, Seoul, Korea

H.Y. Jo

Korea University, Seoul, Korea

S. Choi, D. Gyun, B. Hong, M. Jo, H. Kim, T.J. Kim, K.S. Lee, D.H. Moon, S.K. Park, E. Seo, K.S. Sim

University of Seoul, Seoul, Korea

M. Choi, S. Kang, H. Kim, J.H. Kim, C. Park, I.C. Park, S. Park, G. Ryu

Sungkyunkwan University, Suwon, Korea

Y. Cho, Y. Choi, Y.K. Choi, J. Goh, M.S. Kim, B. Lee, J. Lee, S. Lee, H. Seo, I. Yu

Vilnius University, Vilnius, Lithuania

M.J. Bilinskas, I. Grigelionis, M. Janulis, D. Martisiute, P. Petrov, M. Polujanskas, T. Sabonis

Centro de Investigacion y de Estudios Avanzados del IPN, Mexico City, Mexico

H. Castilla-Valdez, E. De La Cruz-Burelo, I. Heredia-de La Cruz, R. Lopez-Fernandez, R. Magaña Villalba, J. Martínez-Ortega, A. Sánchez-Hernández, L.M. Villasenor-Cendejas

JHEP02(2012)011

Universidad Iberoamericana, Mexico City, Mexico

S. Carrillo Moreno, F. Vazquez Valencia

Benemerita Universidad Autonoma de Puebla, Puebla, Mexico

H.A. Salazar Ibarguen

Universidad Autónoma de San Luis Potosí, San Luis Potosí, Mexico

E. Casimiro Linares, A. Morelos Pineda, M.A. Reyes-Santos

University of Auckland, Auckland, New Zealand

D. Krofcheck, J. Tam

University of Canterbury, Christchurch, New Zealand

A.J. Bell, P.H. Butler, R. Doesburg, H. Silverwood, N. Tambe

National Centre for Physics, Quaid-I-Azam University, Islamabad, Pakistan

M. Ahmad, M.I. Asghar, H.R. Hoorani, S. Khalid, W.A. Khan, T. Khurshid, S. Qazi, M.A. Shah, M. Shoaib

Institute of Experimental Physics, Faculty of Physics, University of Warsaw, Warsaw, Poland

G. Brona, M. Cwiok, W. Dominik, K. Doroba, A. Kalinowski, M. Konecki, J. Krolikowski

Soltan Institute for Nuclear Studies, Warsaw, Poland

T. Frueboes, R. Gokieli, M. Górski, M. Kazana, K. Nawrocki, K. Romanowska-Rybinska, M. Szleper, G. Wrochna, P. Zalewski

Laboratório de Instrumentação e Física Experimental de Partículas, Lisboa, Portugal

N. Almeida, P. Bargassa, A. David, P. Faccioli, P.G. Ferreira Parracho, M. Gallinaro, P. Musella, A. Nayak, J. Pela[1], P.Q. Ribeiro, J. Seixas, J. Varela

Joint Institute for Nuclear Research, Dubna, Russia

S. Afanasiev, I. Belotelov, P. Bunin, M. Gavrilenko, I. Golutvin, I. Gorbunov, A. Kamenev, V. Karjavin, G. Kozlov, A. Lanev, P. Moisenz, V. Palichik, V. Perelygin, S. Shmatov, V. Smirnov, A. Volodko, A. Zarubin

Petersburg Nuclear Physics Institute, Gatchina (St Petersburg), Russia

S. Evstyukhin, V. Golovtsov, Y. Ivanov, V. Kim, P. Levchenko, V. Murzin, V. Oreshkin, I. Smirnov, V. Sulimov, L. Uvarov, S. Vavilov, A. Vorobyev, An. Vorobyev

JHEP02(2012)011

Institute for Nuclear Research, Moscow, Russia

Yu. Andreev, A. Dermenev, S. Gninenko, N. Golubev, M. Kirsanov, N. Krasnikov, V. Matveev, A. Pashenkov, A. Toropin, S. Troitsky

Institute for Theoretical and Experimental Physics, Moscow, Russia

V. Epshteyn, M. Erofeeva, V. Gavrilov, V. Kaftanov†, M. Kossov[1], A. Krokhotin, N. Lychkovskaya, V. Popov, G. Safronov, S. Semenov, V. Stolin, E. Vlasov, A. Zhokin

Moscow State University, Moscow, Russia

A. Belyaev, E. Boos, M. Dubinin[4], L. Dudko, A. Gribushin, V. Klyukhin, O. Kodolova, I. Lokhtin, A. Markina, S. Obraztsov, M. Perfilov, S. Petrushanko, L. Sarycheva, V. Savrin, A. Snigirev

P.N. Lebedev Physical Institute, Moscow, Russia

V. Andreev, M. Azarkin, I. Dremin, M. Kirakosyan, A. Leonidov, G. Mesyats, S.V. Rusakov, A. Vinogradov

State Research Center of Russian Federation, Institute for High Energy Physics, Protvino, Russia

I. Azhgirey, I. Bayshev, S. Bitioukov, V. Grishin[1], V. Kachanov, D. Konstantinov, A. Korablev, V. Krychkine, V. Petrov, R. Ryutin, A. Sobol, L. Tourtchanovitch, S. Troshin, N. Tyurin, A. Uzunian, A. Volkov

University of Belgrade, Faculty of Physics and Vinca Institute of Nuclear Sciences, Belgrade, Serbia

P. Adzic[27], M. Djordjevic, M. Ekmedzic, D. Krpic[27], J. Milosevic

Centro de Investigaciones Energéticas Medioambientales y Tecnológicas (CIEMAT), Madrid, Spain

M. Aguilar-Benitez, J. Alcaraz Maestre, P. Arce, C. Battilana, E. Calvo, M. Cerrada, M. Chamizo Llatas, N. Colino, B. De La Cruz, A. Delgado Peris, C. Diez Pardos, D. Domínguez Vázquez, C. Fernandez Bedoya, J.P. Fernández Ramos, A. Ferrando, J. Flix, M.C. Fouz, P. Garcia-Abia, O. Gonzalez Lopez, S. Goy Lopez, J.M. Hernandez, M.I. Josa, G. Merino, J. Puerta Pelayo, I. Redondo, L. Romero, J. Santaolalla, M.S. Soares, C. Willmott

Universidad Autónoma de Madrid, Madrid, Spain

C. Albajar, G. Codispoti, J.F. de Trocóniz

Universidad de Oviedo, Oviedo, Spain

J. Cuevas, J. Fernandez Menendez, S. Folgueras, I. Gonzalez Caballero, L. Lloret Iglesias, J.M. Vizan Garcia

JHEP02(2012)011

Instituto de Física de Cantabria (IFCA), CSIC-Universidad de Cantabria, Santander, Spain

J.A. Brochero Cifuentes, I.J. Cabrillo, A. Calderon, S.H. Chuang, J. Duarte Campderros, M. Felcini[28], M. Fernandez, G. Gomez, J. Gonzalez Sanchez, C. Jorda, P. Lobelle Pardo, A. Lopez Virto, J. Marco, R. Marco, C. Martinez Rivero, F. Matorras, F.J. Munoz Sanchez, J. Piedra Gomez[29], T. Rodrigo, A.Y. Rodríguez-Marrero, A. Ruiz-Jimeno, L. Scodellaro, M. Sobron Sanudo, I. Vila, R. Vilar Cortabitarte

CERN, European Organization for Nuclear Research, Geneva, Switzerland

D. Abbaneo, E. Auffray, G. Auzinger, P. Baillon, A.H. Ball, D. Barney, C. Bernet[5], W. Bialas, P. Bloch, A. Bocci, H. Breuker, K. Bunkowski, T. Camporesi, G. Cerminara, T. Christiansen, J.A. Coarasa Perez, B. Curé, D. D'Enterria, A. De Roeck, S. Di Guida, M. Dobson, N. Dupont-Sagorin, A. Elliott-Peisert, B. Frisch, W. Funk, A. Gaddi, G. Georgiou, H. Gerwig, D. Gigi, K. Gill, D. Giordano, F. Glege, R. Gomez-Reino Garrido, M. Gouzevitch, P. Govoni, S. Gowdy, R. Guida, L. Guiducci, S. Gundacker, M. Hansen, C. Hartl, J. Harvey, J. Hegeman, B. Hegner, H.F. Hoffmann, V. Innocente, P. Janot, K. Kaadze, E. Karavakis, P. Lecoq, P. Lenzi, C. Lourenço, T. Mäki, M. Malberti, L. Malgeri, M. Mannelli, L. Masetti, G. Mavromanolakis, F. Meijers, S. Mersi, E. Meschi, R. Moser, M.U. Mozer, M. Mulders, E. Nesvold, M. Nguyen, T. Orimoto, L. Orsini, E. Palencia Cortezon, E. Perez, A. Petrilli, A. Pfeiffer, M. Pierini, M. Pimiä, D. Piparo, G. Polese, L. Quertenmont, A. Racz, W. Reece, J. Rodrigues Antunes, G. Rolandi[30], T. Rommerskirchen, C. Rovelli[31], M. Rovere, H. Sakulin, F. Santanastasio, C. Schäfer, C. Schwick, I. Segoni, A. Sharma, P. Siegrist, P. Silva, M. Simon, P. Sphicas[32], D. Spiga, M. Spiropulu[4], M. Stoye, A. Tsirou, P. Vichoudis, H.K. Wöhri, S.D. Worm[33], W.D. Zeuner

Paul Scherrer Institut, Villigen, Switzerland

W. Bertl, K. Deiters, W. Erdmann, K. Gabathuler, R. Horisberger, Q. Ingram, H.C. Kaestli, S. König, D. Kotlinski, U. Langenegger, F. Meier, D. Renker, T. Rohe, J. Sibille[34]

Institute for Particle Physics, ETH Zurich, Zurich, Switzerland

L. Bäni, P. Bortignon, B. Casal, N. Chanon, Z. Chen, S. Cittolin, A. Deisher, G. Dissertori, M. Dittmar, J. Eugster, K. Freudenreich, C. Grab, P. Lecomte, W. Lustermann, C. Marchica[35], P. Martinez Ruiz del Arbol, P. Milenovic[36], N. Mohr, F. Moortgat, C. Nägeli[35], P. Nef, F. Nessi-Tedaldi, L. Pape, F. Pauss, M. Peruzzi, F.J. Ronga, M. Rossini, L. Sala, A.K. Sanchez, M.-C. Sawley, A. Starodumov[37], B. Stieger, M. Takahashi, L. Tauscher†, A. Thea, K. Theofilatos, D. Treille, C. Urscheler, R. Wallny, M. Weber, L. Wehrli, J. Weng

Universität Zürich, Zurich, Switzerland

E. Aguilo, C. Amsler, V. Chiochia, S. De Visscher, C. Favaro, M. Ivova Rikova, B. Millan Mejias, P. Otiougova, P. Robmann, A. Schmidt, H. Snoek, M. Verzetti

JHEP02(2012)011

National Central University, Chung-Li, Taiwan

Y.H. Chang, K.H. Chen, C.M. Kuo, S.W. Li, W. Lin, Z.K. Liu, Y.J. Lu, D. Mekterovic, R. Volpe, S.S. Yu

National Taiwan University (NTU), Taipei, Taiwan

P. Bartalini, P. Chang, Y.H. Chang, Y.W. Chang, Y. Chao, K.F. Chen, C. Dietz, U. Grundler, W.-S. Hou, Y. Hsiung, K.Y. Kao, Y.J. Lei, R.-S. Lu, J.G. Shiu, Y.M. Tzeng, X. Wan, M. Wang

Cukurova University, Adana, Turkey

A. Adiguzel, M.N. Bakirci[38], S. Cerci[39], C. Dozen, I. Dumanoglu, E. Eskut, S. Girgis, G. Gokbulut, I. Hos, E.E. Kangal, A. Kayis Topaksu, G. Onengut, K. Ozdemir, S. Ozturk[40], A. Polatoz, K. Sogut[41], D. Sunar Cerci[39], B. Tali[39], H. Topakli[38], D. Uzun, L.N. Vergili, M. Vergili

Middle East Technical University, Physics Department, Ankara, Turkey

I.V. Akin, T. Aliev, B. Bilin, S. Bilmis, M. Deniz, H. Gamsizkan, A.M. Guler, K. Ocalan, A. Ozpineci, M. Serin, R. Sever, U.E. Surat, M. Yalvac, E. Yildirim, M. Zeyrek

Bogazici University, Istanbul, Turkey

M. Deliomeroglu, E. Gülmez, B. Isildak, M. Kaya[42], O. Kaya[42], M. Özbek, S. Ozkorucuklu[43], N. Sonmez[44]

National Scientific Center, Kharkov Institute of Physics and Technology, Kharkov, Ukraine

L. Levchuk

University of Bristol, Bristol, United Kingdom

F. Bostock, J.J. Brooke, E. Clement, D. Cussans, R. Frazier, J. Goldstein, M. Grimes, G.P. Heath, H.F. Heath, L. Kreczko, S. Metson, D.M. Newbold[33], K. Nirunpong, A. Poll, S. Senkin, V.J. Smith

Rutherford Appleton Laboratory, Didcot, United Kingdom

L. Basso[45], K.W. Bell, A. Belyaev[45], C. Brew, R.M. Brown, B. Camanzi, D.J.A. Cockerill, J.A. Coughlan, K. Harder, S. Harper, J. Jackson, B.W. Kennedy, E. Olaiya, D. Petyt, B.C. Radburn-Smith, C.H. Shepherd-Themistocleous, I.R. Tomalin, W.J. Womersley

Imperial College, London, United Kingdom

R. Bainbridge, G. Ball, J. Ballin, R. Beuselinck, O. Buchmuller, D. Colling, N. Cripps, M. Cutajar, G. Davies, M. Della Negra, W. Ferguson, J. Fulcher, D. Futyan, A. Gilbert, A. Guneratne Bryer, G. Hall, Z. Hatherell, J. Hays, G. Iles, M. Jarvis, G. Karapostoli, L. Lyons, A.-M. Magnan, J. Marrouche, B. Mathias, R. Nandi, J. Nash, A. Nikitenko[37],

JHEP02(2012)011

A. Papageorgiou, M. Pesaresi, K. Petridis, M. Pioppi[46], D.M. Raymond, S. Rogerson, N. Rompotis, A. Rose, M.J. Ryan, C. Seez, P. Sharp, A. Sparrow, A. Tapper, S. Tourneur, M. Vazquez Acosta, T. Virdee, S. Wakefield, N. Wardle, D. Wardrope, T. Whyntie

Brunel University, Uxbridge, United Kingdom

M. Barrett, M. Chadwick, J.E. Cole, P.R. Hobson, A. Khan, P. Kyberd, D. Leslie, W. Martin, I.D. Reid, L. Teodorescu

Baylor University, Waco, USA

K. Hatakeyama, H. Liu

The University of Alabama, Tuscaloosa, USA

C. Henderson

Boston University, Boston, USA

A. Avetisyan, T. Bose, E. Carrera Jarrin, C. Fantasia, A. Heister, J. St. John, P. Lawson, D. Lazic, J. Rohlf, D. Sperka, L. Sulak

Brown University, Providence, USA

S. Bhattacharya, D. Cutts, A. Ferapontov, U. Heintz, S. Jabeen, G. Kukartsev, G. Landsberg, M. Luk, M. Narain, D. Nguyen, M. Segala, T. Sinthuprasith, T. Speer, K.V. Tsang

University of California, Davis, Davis, USA

R. Breedon, G. Breto, M. Calderon De La Barca Sanchez, S. Chauhan, M. Chertok, J. Conway, R. Conway, P.T. Cox, J. Dolen, R. Erbacher, R. Houtz, W. Ko, A. Kopecky, R. Lander, H. Liu, O. Mall, S. Maruyama, T. Miceli, D. Pellett, J. Robles, B. Rutherford, M. Searle, J. Smith, M. Squires, M. Tripathi, R. Vasquez Sierra

University of California, Los Angeles, Los Angeles, USA

V. Andreev, K. Arisaka, D. Cline, R. Cousins, J. Duris, S. Erhan, P. Everaerts, C. Farrell, J. Hauser, M. Ignatenko, C. Jarvis, C. Plager, G. Rakness, P. Schlein†, J. Tucker, V. Valuev

University of California, Riverside, Riverside, USA

J. Babb, R. Clare, J. Ellison, J.W. Gary, F. Giordano, G. Hanson, G.Y. Jeng, S.C. Kao, H. Liu, O.R. Long, A. Luthra, H. Nguyen, S. Paramesvaran, J. Sturdy, S. Sumowidagdo, R. Wilken, S. Wimpenny

University of California, San Diego, La Jolla, USA

W. Andrews, J.G. Branson, G.B. Cerati, D. Evans, F. Golf, A. Holzner, M. Lebourgeois, J. Letts, B. Mangano, S. Padhi, C. Palmer, G. Petrucciani, H. Pi, M. Pieri, R. Ranieri, M. Sani, V. Sharma, S. Simon, E. Sudano, M. Tadel, Y. Tu, A. Vartak, S. Wasserbaech[47], F. Würthwein, A. Yagil, J. Yoo

JHEP02(2012)011

University of California, Santa Barbara, Santa Barbara, USA

D. Barge, R. Bellan, C. Campagnari, M. D'Alfonso, T. Danielson, K. Flowers, P. Geffert, C. George, J. Incandela, C. Justus, P. Kalavase, S.A. Koay, D. Kovalskyi[1], V. Krutelyov, S. Lowette, N. Mccoll, S.D. Mullin, V. Pavlunin, F. Rebassoo, J. Ribnik, J. Richman, R. Rossin, D. Stuart, W. To, J.R. Vlimant, C. West

California Institute of Technology, Pasadena, USA

A. Apresyan, A. Bornheim, J. Bunn, Y. Chen, E. Di Marco, J. Duarte, M. Gataullin, Y. Ma, A. Mott, H.B. Newman, C. Rogan, V. Timciuc, P. Traczyk, J. Veverka, R. Wilkinson, Y. Yang, R.Y. Zhu

Carnegie Mellon University, Pittsburgh, USA

B. Akgun, R. Carroll, T. Ferguson, Y. Iiyama, D.W. Jang, S.Y. Jun, Y.F. Liu, M. Paulini, J. Russ, H. Vogel, I. Vorobiev

University of Colorado at Boulder, Boulder, USA

J.P. Cumalat, M.E. Dinardo, B.R. Drell, C.J. Edelmaier, W.T. Ford, A. Gaz, B. Heyburn, E. Luiggi Lopez, U. Nauenberg, J.G. Smith, K. Stenson, K.A. Ulmer, S.R. Wagner, S.L. Zang

Cornell University, Ithaca, USA

L. Agostino, J. Alexander, A. Chatterjee, N. Eggert, L.K. Gibbons, B. Heltsley, W. Hopkins, A. Khukhunaishvili, B. Kreis, G. Nicolas Kaufman, J.R. Patterson, D. Puigh, A. Ryd, E. Salvati, X. Shi, W. Sun, W.D. Teo, J. Thom, J. Thompson, J. Vaughan, Y. Weng, L. Winstrom, P. Wittich

Fairfield University, Fairfield, USA

A. Biselli, G. Cirino, D. Winn

Fermi National Accelerator Laboratory, Batavia, USA

S. Abdullin, M. Albrow, J. Anderson, G. Apollinari, M. Atac, J.A. Bakken, L.A.T. Bauerdick, A. Beretvas, J. Berryhill, P.C. Bhat, I. Bloch, K. Burkett, J.N. Butler, V. Chetluru, H.W.K. Cheung, F. Chlebana, S. Cihangir, W. Cooper, D.P. Eartly, V.D. Elvira, S. Esen, I. Fisk, J. Freeman, Y. Gao, E. Gottschalk, D. Green, O. Gutsche, J. Hanlon, R.M. Harris, J. Hirschauer, B. Hooberman, H. Jensen, S. Jindariani, M. Johnson, U. Joshi, B. Klima, K. Kousouris, S. Kunori, S. Kwan, C. Leonidopoulos, D. Lincoln, R. Lipton, J. Lykken, K. Maeshima, J.M. Marraffino, D. Mason, P. McBride, T. Miao, K. Mishra, S. Mrenna, Y. Musienko[48], C. Newman-Holmes, V. O'Dell, J. Pivarski, R. Pordes, O. Prokofyev, T. Schwarz, E. Sexton-Kennedy, S. Sharma, W.J. Spalding, L. Spiegel, P. Tan, L. Taylor, S. Tkaczyk, L. Uplegger, E.W. Vaandering, R. Vidal, J. Whitmore, W. Wu, F. Yang, F. Yumiceva, J.C. Yun

JHEP02(2012)011

University of Florida, Gainesville, USA

D. Acosta, P. Avery, D. Bourilkov, M. Chen, S. Das, M. De Gruttola, G.P. Di Giovanni, D. Dobur, A. Drozdetskiy, R.D. Field, M. Fisher, Y. Fu, I.K. Furic, J. Gartner, S. Goldberg, J. Hugon, B. Kim, J. Konigsberg, A. Korytov, A. Kropivnitskaya, T. Kypreos, J.F. Low, K. Matchev, G. Mitselmakher, L. Muniz, P. Myeonghun, R. Remington, A. Rinkevicius, M. Schmitt, B. Scurlock, P. Sellers, N. Skhirtladze, M. Snowball, D. Wang, J. Yelton, M. Zakaria

Florida International University, Miami, USA

V. Gaultney, L.M. Lebolo, S. Linn, P. Markowitz, G. Martinez, J.L. Rodriguez

Florida State University, Tallahassee, USA

T. Adams, A. Askew, J. Bochenek, J. Chen, B. Diamond, S.V. Gleyzer, J. Haas, S. Hagopian, V. Hagopian, M. Jenkins, K.F. Johnson, H. Prosper, S. Sekmen, V. Veeraraghavan

Florida Institute of Technology, Melbourne, USA

M.M. Baarmand, B. Dorney, M. Hohlmann, H. Kalakhety, I. Vodopiyanov

University of Illinois at Chicago (UIC), Chicago, USA

M.R. Adams, I.M. Anghel, L. Apanasevich, Y. Bai, V.E. Bazterra, R.R. Betts, J. Callner, R. Cavanaugh, C. Dragoiu, L. Gauthier, C.E. Gerber, D.J. Hofman, S. Khalatyan, G.J. Kunde[49], F. Lacroix, M. Malek, C. O'Brien, C. Silkworth, C. Silvestre, D. Strom, N. Varelas

The University of Iowa, Iowa City, USA

U. Akgun, E.A. Albayrak, B. Bilki, W. Clarida, F. Duru, S. Griffiths, C.K. Lae, E. McCliment, J.-P. Merlo, H. Mermerkaya[50], A. Mestvirishvili, A. Moeller, J. Nachtman, C.R. Newsom, E. Norbeck, J. Olson, Y. Onel, F. Ozok, S. Sen, J. Wetzel, T. Yetkin, K. Yi

Johns Hopkins University, Baltimore, USA

B.A. Barnett, B. Blumenfeld, S. Bolognesi, A. Bonato, C. Eskew, D. Fehling, G. Giurgiu, A.V. Gritsan, Z.J. Guo, G. Hu, P. Maksimovic, S. Rappoccio, M. Swartz, N.V. Tran, A. Whitbeck

The University of Kansas, Lawrence, USA

P. Baringer, A. Bean, G. Benelli, O. Grachov, R.P. Kenny Iii, M. Murray, D. Noonan, S. Sanders, R. Stringer, J.S. Wood, V. Zhukova

Kansas State University, Manhattan, USA

A.F. Barfuss, T. Bolton, I. Chakaberia, A. Ivanov, S. Khalil, M. Makouski, Y. Maravin, S. Shrestha, I. Svintradze

JHEP02(2012)011

Lawrence Livermore National Laboratory, Livermore, USA

J. Gronberg, D. Lange, D. Wright

University of Maryland, College Park, USA

A. Baden, M. Boutemeur, S.C. Eno, J.A. Gomez, N.J. Hadley, R.G. Kellogg, M. Kirn, Y. Lu, A.C. Mignerey, K. Rossato, P. Rumerio, A. Skuja, J. Temple, M.B. Tonjes, S.C. Tonwar, E. Twedt

Massachusetts Institute of Technology, Cambridge, USA

B. Alver, G. Bauer, J. Bendavid, W. Busza, E. Butz, I.A. Cali, M. Chan, V. Dutta, G. Gomez Ceballos, M. Goncharov, K.A. Hahn, P. Harris, Y. Kim, M. Klute, Y.-J. Lee, W. Li, P.D. Luckey, T. Ma, S. Nahn, C. Paus, D. Ralph, C. Roland, G. Roland, M. Rudolph, G.S.F. Stephans, F. Stöckli, K. Sumorok, K. Sung, D. Velicanu, E.A. Wenger, R. Wolf, B. Wyslouch, S. Xie, M. Yang, Y. Yilmaz, A.S. Yoon, M. Zanetti

University of Minnesota, Minneapolis, USA

S.I. Cooper, P. Cushman, B. Dahmes, A. De Benedetti, G. Franzoni, A. Gude, J. Haupt, K. Klapoetke, Y. Kubota, J. Mans, N. Pastika, V. Rekovic, R. Rusack, M. Sasseville, A. Singovsky, J. Turkewitz

University of Mississippi, University, USA

L.M. Cremaldi, R. Godang, R. Kroeger, L. Perera, R. Rahmat, D.A. Sanders, D. Summers

University of Nebraska-Lincoln, Lincoln, USA

E. Avdeeva, K. Bloom, S. Bose, J. Butt, D.R. Claes, A. Dominguez, M. Eads, P. Jindal, J. Keller, I. Kravchenko, J. Lazo-Flores, H. Malbouisson, S. Malik, G.R. Snow

State University of New York at Buffalo, Buffalo, USA

U. Baur, A. Godshalk, I. Iashvili, S. Jain, A. Kharchilava, A. Kumar, K. Smith, Z. Wan

Northeastern University, Boston, USA

G. Alverson, E. Barberis, D. Baumgartel, M. Chasco, S. Reucroft, D. Trocino, D. Wood, J. Zhang

Northwestern University, Evanston, USA

A. Anastassov, A. Kubik, N. Mucia, N. Odell, R.A. Ofierzynski, B. Pollack, A. Pozdnyakov, M. Schmitt, S. Stoynev, M. Velasco, S. Won

University of Notre Dame, Notre Dame, USA

L. Antonelli, D. Berry, A. Brinkerhoff, M. Hildreth, C. Jessop, D.J. Karmgard, J. Kolb, T. Kolberg, K. Lannon, W. Luo, S. Lynch, N. Marinelli, D.M. Morse, T. Pearson, R. Ruchti, J. Slaunwhite, N. Valls, M. Wayne, J. Ziegler

JHEP02(2012)011

The Ohio State University, Columbus, USA

B. Bylsma, L.S. Durkin, C. Hill, P. Killewald, K. Kotov, T.Y. Ling, M. Rodenburg, C. Vuosalo, G. Williams

Princeton University, Princeton, USA

N. Adam, E. Berry, P. Elmer, D. Gerbaudo, V. Halyo, P. Hebda, A. Hunt, E. Laird, D. Lopes Pegna, P. Lujan, D. Marlow, T. Medvedeva, M. Mooney, J. Olsen, P. Piroué, X. Quan, A. Raval, H. Saka, D. Stickland, C. Tully, J.S. Werner, A. Zuranski

University of Puerto Rico, Mayaguez, USA

J.G. Acosta, X.T. Huang, A. Lopez, H. Mendez, S. Oliveros, J.E. Ramirez Vargas, A. Zatserklyaniy

Purdue University, West Lafayette, USA

E. Alagoz, V.E. Barnes, D. Benedetti, G. Bolla, L. Borrello, D. Bortoletto, M. De Mattia, A. Everett, L. Gutay, Z. Hu, M. Jones, O. Koybasi, M. Kress, A.T. Laasanen, N. Leonardo, V. Maroussov, P. Merkel, D.H. Miller, N. Neumeister, I. Shipsey, D. Silvers, A. Svyatkovskiy, M. Vidal Marono, H.D. Yoo, J. Zablocki, Y. Zheng

Purdue University Calumet, Hammond, USA

S. Guragain, N. Parashar

Rice University, Houston, USA

A. Adair, C. Boulahouache, V. Cuplov, K.M. Ecklund, F.J.M. Geurts, B.P. Padley, R. Redjimi, J. Roberts, J. Zabel

University of Rochester, Rochester, USA

B. Betchart, A. Bodek, Y.S. Chung, R. Covarelli, P. de Barbaro, R. Demina, Y. Eshaq, H. Flacher, A. Garcia-Bellido, P. Goldenzweig, Y. Gotra, J. Han, A. Harel, D.C. Miner, G. Petrillo, W. Sakumoto, D. Vishnevskiy, M. Zielinski

The Rockefeller University, New York, USA

A. Bhatti, R. Ciesielski, L. Demortier, K. Goulianos, G. Lungu, S. Malik, C. Mesropian

Rutgers, the State University of New Jersey, Piscataway, USA

S. Arora, O. Atramentov, A. Barker, J.P. Chou, C. Contreras-Campana, E. Contreras-Campana, D. Duggan, D. Ferencek, Y. Gershtein, R. Gray, E. Halkiadakis, D. Hidas, D. Hits, A. Lath, S. Panwalkar, M. Park, R. Patel, A. Richards, K. Rose, S. Salur, S. Schnetzer, S. Somalwar, R. Stone, S. Thomas

University of Tennessee, Knoxville, USA

G. Cerizza, M. Hollingsworth, S. Spanier, Z.C. Yang, A. York

JHEP02(2012)011

Texas A&M University, College Station, USA

R. Eusebi, W. Flanagan, J. Gilmore, A. Gurrola, T. Kamon[51], V. Khotilovich, R. Montalvo, I. Osipenkov, Y. Pakhotin, A. Perloff, J. Roe, A. Safonov, S. Sengupta, I. Suarez, A. Tatarinov, D. Toback

Texas Tech University, Lubbock, USA

N. Akchurin, C. Bardak, J. Damgov, P.R. Dudero, C. Jeong, K. Kovitanggoon, S.W. Lee, T. Libeiro, P. Mane, Y. Roh, A. Sill, I. Volobouev, R. Wigmans, E. Yazgan

Vanderbilt University, Nashville, USA

E. Appelt, E. Brownson, D. Engh, C. Florez, W. Gabella, M. Issah, W. Johns, C. Johnston, P. Kurt, C. Maguire, A. Melo, P. Sheldon, B. Snook, S. Tuo, J. Velkovska

University of Virginia, Charlottesville, USA

M.W. Arenton, M. Balazs, S. Boutle, S. Conetti, B. Cox, B. Francis, S. Goadhouse, J. Goodell, R. Hirosky, A. Ledovskoy, C. Lin, C. Neu, J. Wood, R. Yohay

Wayne State University, Detroit, USA

S. Gollapinni, R. Harr, P.E. Karchin, C. Kottachchi Kankanamge Don, P. Lamichhane, M. Mattson, C. Milstène, A. Sakharov

University of Wisconsin, Madison, USA

M. Anderson, M. Bachtis, D. Belknap, J.N. Bellinger, D. Carlsmith, M. Cepeda, S. Dasu, J. Efron, E. Friis, L. Gray, K.S. Grogg, M. Grothe, R. Hall-Wilton, M. Herndon, A. Hervé, P. Klabbers, J. Klukas, A. Lanaro, C. Lazaridis, J. Leonard, R. Loveless, A. Mohapatra, I. Ojalvo, W. Parker, G.A. Pierro, I. Ross, A. Savin, W.H. Smith, J. Swanson, M. Weinberg

JHEP02(2012)011

†: Deceased
1: Also at CERN, European Organization for Nuclear Research, Geneva, Switzerland
2: Also at National Institute of Chemical Physics and Biophysics, Tallinn, Estonia
3: Also at Universidade Federal do ABC, Santo Andre, Brazil
4: Also at California Institute of Technology, Pasadena, USA
5: Also at Laboratoire Leprince-Ringuet, Ecole Polytechnique, IN2P3-CNRS, Palaiseau, France
6: Also at Suez Canal University, Suez, Egypt
7: Also at Cairo University, Cairo, Egypt
8: Also at British University, Cairo, Egypt
9: Also at Fayoum University, El-Fayoum, Egypt
10: Also at Ain Shams University, Cairo, Egypt
11: Also at Soltan Institute for Nuclear Studies, Warsaw, Poland
12: Also at Université de Haute-Alsace, Mulhouse, France
13: Also at Moscow State University, Moscow, Russia
14: Also at Brandenburg University of Technology, Cottbus, Germany
15: Also at Institute of Nuclear Research ATOMKI, Debrecen, Hungary
16: Also at Eötvös Loránd University, Budapest, Hungary
17: Also at Tata Institute of Fundamental Research - HECR, Mumbai, India
18: Also at University of Visva-Bharati, Santiniketan, India
19: Also at Sharif University of Technology, Tehran, Iran
20: Also at Isfahan University of Technology, Isfahan, Iran
21: Also at Shiraz University, Shiraz, Iran
22: Also at Plasma Physics Research Center, Islamic Azad University, Teheran, Iran
23: Also at Facoltà Ingegneria Università di Roma, Roma, Italy
24: Also at Università della Basilicata, Potenza, Italy
25: Also at Laboratori Nazionali di Legnaro dell' INFN, Legnaro, Italy
26: Also at Università degli studi di Siena, Siena, Italy
27: Also at Faculty of Physics of University of Belgrade, Belgrade, Serbia
28: Also at University of California, Los Angeles, Los Angeles, USA
29: Also at University of Florida, Gainesville, USA
30: Also at Scuola Normale e Sezione dell' INFN, Pisa, Italy
31: Also at INFN Sezione di Roma; Università di Roma "La Sapienza", Roma, Italy
32: Also at University of Athens, Athens, Greece
33: Now at Rutherford Appleton Laboratory, Didcot, United Kingdom
34: Also at The University of Kansas, Lawrence, USA
35: Also at Paul Scherrer Institut, Villigen, Switzerland
36: Also at University of Belgrade, Faculty of Physics and Vinca Institute of Nuclear Sciences, Belgrade, Serbia
37: Also at Institute for Theoretical and Experimental Physics, Moscow, Russia
38: Also at Gaziosmanpasa University, Tokat, Turkey
39: Also at Adiyaman University, Adiyaman, Turkey
40: Also at The University of Iowa, Iowa City, USA
41: Also at Mersin University, Mersin, Turkey
42: Also at Kafkas University, Kars, Turkey
43: Also at Suleyman Demirel University, Isparta, Turkey
44: Also at Ege University, Izmir, Turkey
45: Also at School of Physics and Astronomy, University of Southampton, Southampton, United Kingdom
46: Also at INFN Sezione di Perugia; Università di Perugia, Perugia, Italy
47: Also at Utah Valley University, Orem, USA
48: Also at Institute for Nuclear Research, Moscow, Russia
49: Also at Los Alamos National Laboratory, Los Alamos, USA
50: Also at Erzincan University, Erzincan, Turkey
51: Also at Kyungpook National University, Daegu, Korea

JHEP02(2012)011